iScience

CellPress
OPEN ACCESS

Article

Corosolic acid attenuates cardiac ischemia/reperfusion injury through the PHB2/PINK1/parkin/mitophagy pathway

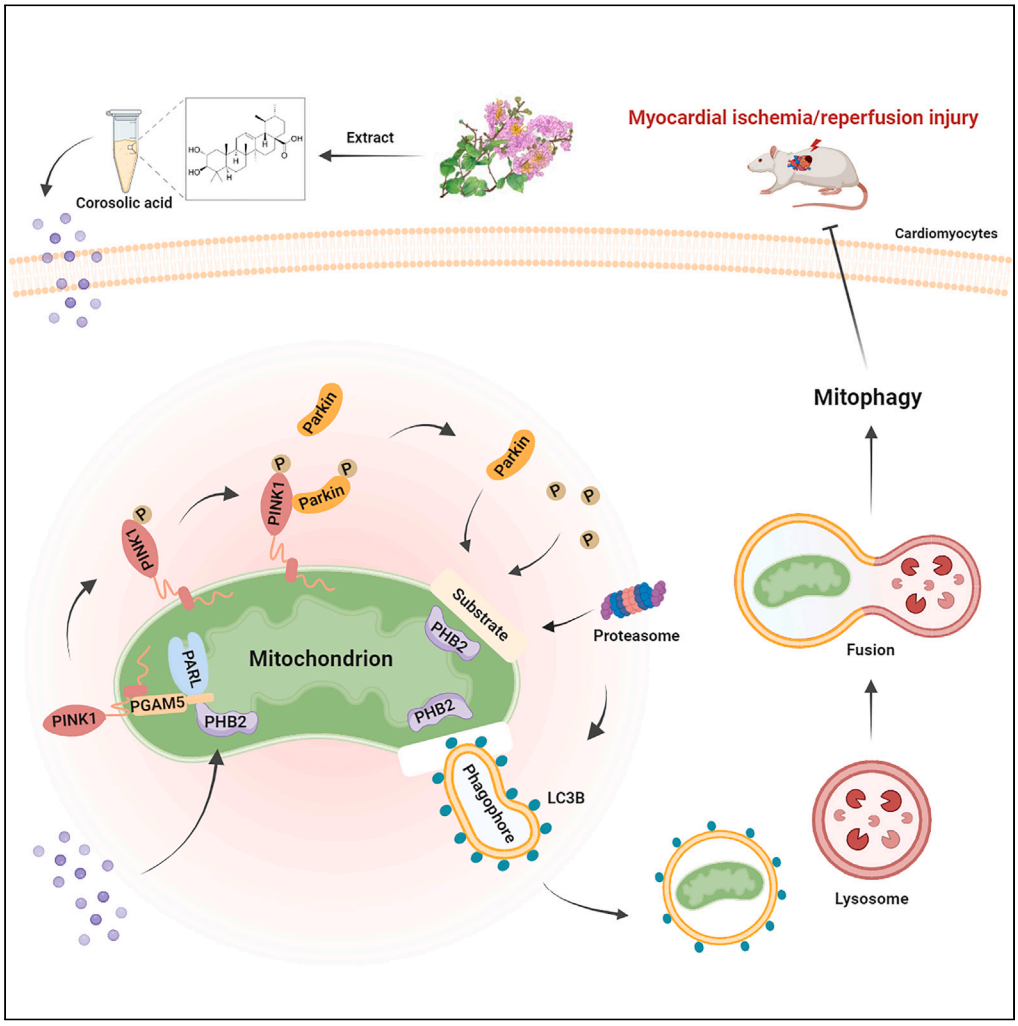

Jun Zhang, Yongjian Zhao, Lin Yan, ..., Tianke Yang, Tingbo Jiang, Hongxia Li

gyytk94@sina.com (T.Y.)
18906201122@189.cn (T.J.)
shrimp@suda.edu.cn (H.L.)

Highlights

Myocardial ischemia-reperfusion injury exhibits reduced mitophagy levels

Corosolic acid alleviates myocardial ischemia-reperfusion injury

PHB2 participates in the regulation of mitophagy by corosolic acid

Zhang et al., iScience 27, 110448
August 16, 2024
https://doi.org/10.1016/j.isci.2024.110448

iScience

CellPress
OPEN ACCESS

Article

Corosolic acid attenuates cardiac ischemia/reperfusion injury through the PHB2/PINK1/parkin/mitophagy pathway

Jun Zhang,[1,3] Yongjian Zhao,[1,3] Lin Yan,[1,3] Mingyue Tan,[1,3] Yifeng Jin,[1] Yunfei Yin,[1] Lianhua Han,[1] Xiao Ma,[1] Yimin Li,[1] Tianke Yang,[2,*] Tingbo Jiang,[1,*] and Hongxia Li[1,4,*]

SUMMARY

Despite advances in treatment, myocardial infarction remains the leading cause of heart failure and death worldwide, and the restoration of coronary blood flow can also cause heart damage. In this study, we found that corosolic acid (CA), also known as plant insulin, significantly protects the heart from ischemia-reperfusion (I/R) injury. In addition, CA can inhibit oxidative stress and improve mitochondrial structure and function in cardiomyocytes. Subsequently, our study demonstrated that CA improved the expression of the mitophagy-related proteins Prohibitin 2 (PHB2), PTEN-induced putative kinase protein-1 (PINK1), and Parkin. Meanwhile, through molecular docking, we found an excellent binding between CA and PHB2 protein. Finally, the knockdown of PHB2 eliminated the protective effect of CA on hypoxia-reoxygenation in cardiomyocytes. Taken together, our study reveals that CA increases mitophagy in cardiomyocytes via the PHB2/PINK1/Parkin signaling pathway, inhibits oxidative stress response, and maintains mitochondrial function, thereby improving cardiac function after I/R.

INTRODUCTION

One of the main causes of death in elderly adults is acute myocardial infarction (AMI), which is brought on by a sudden embolism of the coronary arteries.[1,2] The main clinical strategy for treating myocardial infarction is regarded to be the prompt restoration of blood supply to the ischemic heart. In spite of the fact that the reperfusion strategy was effective in decreasing the mortality associated with AMI, re-introduction of fresh blood often leads to additional harm to the post-ischemic myocardium, which is known as myocardial ischemia-reperfusion (I/R) injury.[3] Cardiomyocyte oxidative stress, apoptosis, and inflammation are primarily linked to cardiac I/R damage and result in malignant arrhythmia and constriction dysfunction.[4–7] To create new therapeutic medications that lessen I/R-induced cardiac injury, greater research into the mechanisms underlying the pathophysiology of myocardial I/R injury is thus required.

Cardiomyocyte function and extracellular damage signals are synchronized by the mitochondria, which account for more than 30% of the total volume of cardiomyocytes.[8,9] Recent observations depicted that mitochondria are crucial to the pathological development of myocardial I/R damage.[10–12] In cardiomyocytes, the rate of oxidative phosphorylation is controlled by mitochondria, which are metabolic organelles.[13] Insufficient energy cannot be produced by abnormal mitochondria to support the needs of heart tissue.[14,15] In addition, mitochondria are also involved in oxidative stress, inflammatory response, calcium homeostasis, autophagy, and cell death.[11,16–19] The capacity of cardiomyocytes to contract and relax is decreased by mild mitochondrial dysfunction because it results in the accumulation of reactive oxygen species (ROS) and affects the synthesis and release of adenosine triphosphate (ATP).[20–22] Severe mitochondrial damage can release pro-apoptotic factors and lead to programmed cell death.[23] Because adult human cardiomyocytes rarely divide, the number of dysfunctional mitochondria cannot be easily diluted by cell division. Therefore, efficient degradation of dysfunctional mitochondria is essential to maintain cellular function.[24]

Mitophagy is an evolutionally conserved cellular process that selectively removes damaged or aging mitochondria through the lysosome pathway, which determines its protective effect on mitochondrial homeostasis and cardiomyocyte apoptosis. In a host of pathophysiological circumstances involving myocardial I/R damage, doxorubicin (DOX)-related myocardial damage, and myocardial damage brought on by diabetic cardiomyopathy, mitophagy has been shown to protect both the structure and the function of cardiomyocytes.[25–27] One of the most well-studied mitophagy mechanisms involves the removal of damaged mitochondria via PTEN-induced putative kinase protein-1 (PINK1)/parkin labeling.[28] In a healthy situation, PINK1, a mitochondrial serine/threonine kinase, is transported to mitochondria and then sheared by the inner membrane protease presenilin-associated rhomboid-like (PARL). Sheared PINK1 is discharged into the cytoplasm, where it is degraded by the proteasome. When mitochondria are damaged, PINK1 cleavage is inhibited. Full-length PINK1 builds up in the mitochondrial outer membrane and attracts parkin, followed by ubiquitination to label damaged mitochondria for selective clearance.[29,30] RhoA, a

[1]Department of Cardiology, The First Affiliated Hospital of Soochow University, 188 Shizi Street, Suzhou, Jiangsu 215006, P.R. China
[2]Department of Ophthalmology, The First Affiliated Hospital of USTC, University of Science and Technology of China, Hefei, P.R. China
[3]These authors contributed equally
[4]Lead contact
*Correspondence: gyytk94@sina.com (T.Y.), 18906201122@189.cn (T.J.), shrimp@suda.edu.cn (H.L.)
https://doi.org/10.1016/j.isci.2024.110448

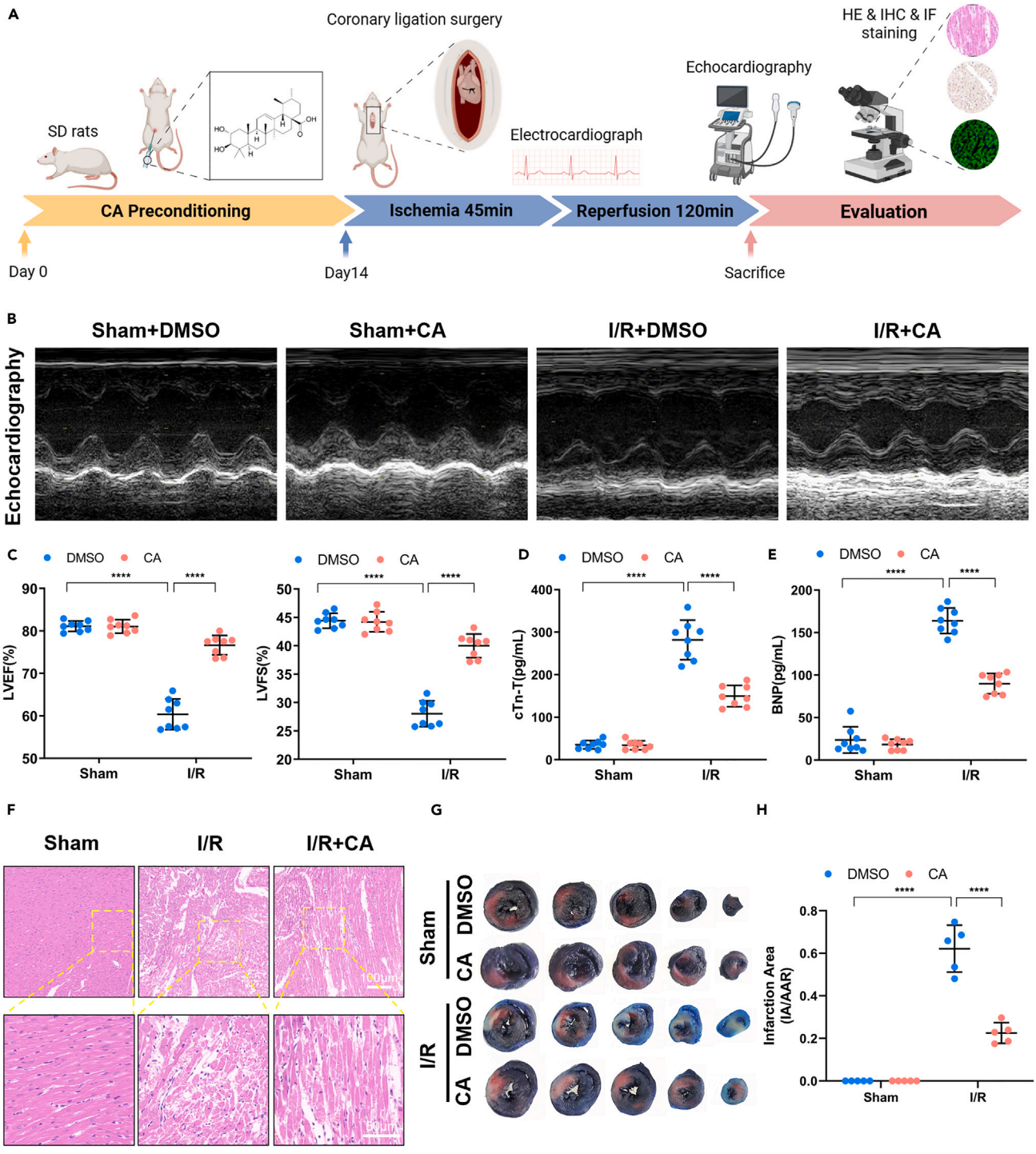

Figure 1. Protective effect of corosolic acid on myocardial I/R injury in rats

Rats were divided into the sham operation group and the myocardial I/R injury group. Rats in the treatment group were given corosolic acid (10 mg/kg/d) 14 days before surgery.

(A) Construction of the animal model and schedule of experimental measurements.

(B) Representative echocardiographic images of rats in each group, $n = 8$.

(C) Analysis of echocardiogram to obtain a quantification of LVEF% and LVFS%, $n = 8$.

(D and E) Determination of cTn-T and BNP content in rat serum, $n = 8$.

(F) Observation of cellular morphology in cardiac tissue using HE staining, $n = 5$.

Figure 1. *Continued*

(G) Heart was stained by TTC/Evans Blue double staining, $n = 5$. The red area represents the dangerous area (TTC staining), the blue area represents the unaffected area (Evans Blue staining), and the white area represents the infarction area.

(H) Quantitative analysis of infarcted area (white): dangerous area (red+white). Experiments were repeated at least three times and the data are shown as mean ± SD. two-way ANOVA was used to compare differences. *$p < 0.05$, **$p < 0.01$, ***$p < 0.001$, ****$p < 0.0001$, ns represent not significant.

small GTPase, promotes the stabilization of PINK1 independently of mitochondrial depolarization in cardiomyocytes, thereby promoting mitophagy and protecting the heart against ischemia.[24,31] Prohibitin 2 (PHB2) is an evolutionarily conserved mitochondrial inner membrane protein. In previous studies, PHB2 was shown to be an inner mitochondrial membrane mitophagy receptor. PHB2 binds the autophagosome membrane-associated protein LC3 via the LC3-interaction region (LIR) domain during mitochondrial depolarization and proteasome-dependent outer membrane rupture.[32] However, recent studies have shown that PHB2 modulates PARL activity, which in turn promotes PINK1/Parkin-mediated mitophagy.[33] In addition, it has been shown that myocardial ischemia will lead to reduced levels of PHB2 in mitochondria. And enforced expression of PHB2 leads to a decrease in mitochondrial fission and apoptosis and improves the area of cardiac infarction after I/R.[34] However, the role of PHB2-mediated mitophagy in myocardial I/R injury remains unclear.

Corosolic acid (CA), a pentacyclic triterpenoid found in the leaves of the Banaba tree (Lagerstroemia speciosa), significantly reduces blood sugar levels.[35] CA has started a phase III clinical pharmacodynamic evaluation for the American Food and Drug Administration (USA) to prevent and treat diabetes.[36] Interestingly, the heart-protective properties of CA have recently gotten a growing attention. For instance, in mice with the ligation of the left anterior descending branch of the coronary artery, CA reduces myocardial infarction-induced heart fibrosis and dysfunction via controlling inflammation and oxidative stress linked to AMPKα. In addition, in a mouse model of pressure overload induced by aortic banding surgery, CA can reduce myocardial hypertrophy by regulating AMPK-dependent autophagy.[37] In the streptozotocin-induced rat diabetes model, CA had a significant ameliorating effect on isoproterenol-induced acute myocardial injury, which was associated with the activation of the peroxisome proliferator-activated receptor gamma (PPAR-γ) pathway.[38] Regarding mitochondrial biology, CA has been found to activate transcription factor EB (TFEB) in an AMPKα2-dependent manner to inhibit mitochondrial oxidative stress induced by DOX and promote ATP production in cardiomyocytes.[39] Based on these results, CA appears to be a viable new target for the treatment of cardiovascular disease. Therefore, we looked into whether CA could shield cardiac I/R damage by maintaining mitochondrial homeostasis. Particularly, we looked at whether CA may activate mitophagy to lessen I/R-induced mitochondrial unbalance in the cardiomyocyte and investigated its molecular mechanisms in I/R damage.

RESULTS

Corosolic acid protected the heart from ischemia-reperfusion-induced injuries

In this experiment, rats were processed according to the time nodes on the animal experiment flow chart (Figure 1A). The results of echocardiography showed that cardiac function was compromised after I/R. Specifically, following CA therapy, both LVFS% and LVEF% elevated (Figures 1B and 1C). Following CA pretreatment, cardiac troponin T (cTn-T) and brain natriuretic peptide (BNP) decreased in accordance with the results of the echocardiogram (Figures 1D and 1E). The results of HE staining in the ischemic area showed that compared with the sham-operated group, the I/R group showed myocardial structural damage, disorganized cell distribution, cell swelling, and vacuole formation. However, CA treatment alleviated the myocardial structural damage caused by I/R. I/R-treated rats had a myocardial structural injury, unordered fiber distribution, decreased myocardial cells, and nuclear shrinkage compared to sham-operated control rats, according to H&E staining of the heart. However, CA prevented these alterations in cardiac muscle tissue (Figure 1F). Additionally, The I/R group had a considerably greater infarct area than the sham group, which may be reversed by CA treatment, according to TTC/Evans Blue double staining (Figures 1G and 1H). Together, these data indicated that CA enhances cardiac function and reduces myocardial I/R injury in rats.

Corosolic acid safeguarded the heart from ischemia-reperfusion-induced mitochondrial dysfunction

Excessive ROS, which are primarily produced by mitochondria, are known to exacerbate mitochondrial dysfunction. We employed an electron microscope to study the mitochondrial ultrastructure of the heart tissue in order to assess the impact of CA on I/R-induced mitochondrial dysfunction. In contrast to control rats who underwent a sham operation, I/R-treated rats typically displayed enlarged mitochondria with scant cristae and empty vacuoles. The complete cristae mitochondriale in the drug-treated group showed that CA blocked these alterations in the mitochondrial ultrastructure (Figures 2A and 2D). Additionally, we noticed that following I/R therapy, there were fewer mitochondria, which could be seen by TOMM20 staining. CA treatments significantly restored the number of mitochondria (Figures 2B and 2E).

Subsequently, we confirmed the impact of CA on apoptosis. TUNEL staining of the ischemic area revealed that apoptosis in the I/R group was much more than that in the sham group, and CA treatment reduced the increase of myocardial apoptosis (Figures 2C and 2F). Furthermore, we measured the amount of ATP present in the tissue to ascertain the contribution of CA to mitochondrial function. In the CA treatment group, the level of ATP was higher than that in the injury group (Figure 2G). In order to assess oxidative stress, we also evaluated the MDA, a product of lipid peroxidation, concentration in the tissue of rats. The content of MDA decreased following CA administration (Figure 2H). These findings imply that CA ameliorates the *in vivo* imbalance in mitochondrial structure and function brought on by I/R.

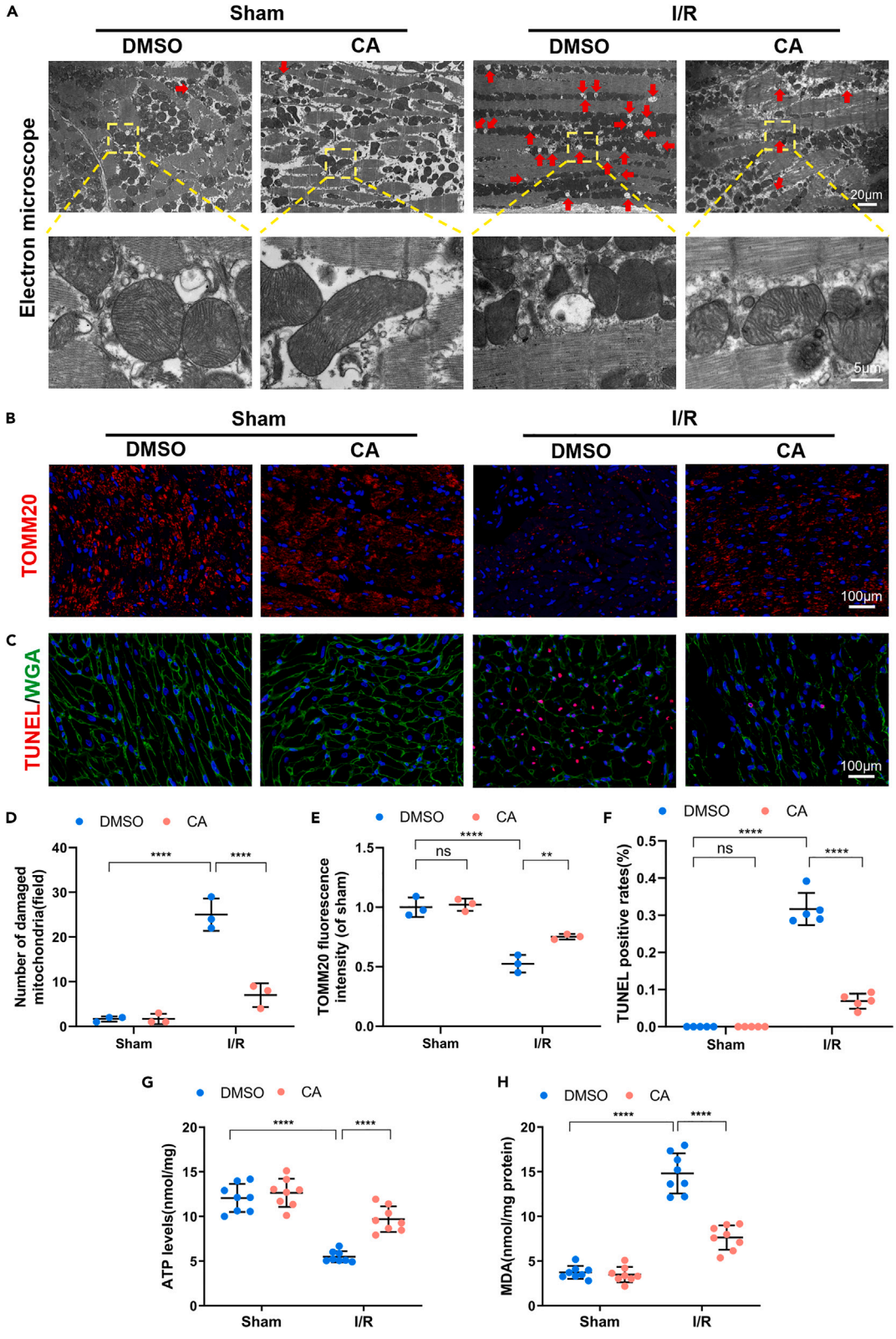
A
Sham
I/R
DMSO
CA
DMSO
CA
Electron microscope
20μm
5μm
B
Sham
I/R
DMSO
CA
DMSO
CA
TOMM20
100μm
C
TUNEL/WGA
100μm
D
DMSO
CA
Number of damaged mitochondria(field)
****
****
Sham
I/R
E
DMSO
CA
TOMM20 fluorescence intensity (of sham)
****
ns
**
Sham
I/R
F
DMSO
CA
TUNEL positive rates(%)
****
ns
****
Sham
I/R
G
DMSO
CA
ATP levels(nmol/mg)
****
****
Sham
I/R
H
DMSO
CA
MDA(nmol/mg protein)
****
****
Sham
I/R

Figure 2. Corosolic acid attenuates cardiac mitochondrial damage induced by I/R

Rats were divided into a sham group and a myocardial I/R injury group with or without CA treatment.

(A and D) The changes of mitochondria in reperfused heart cardiomyocytes were observed by transmission electron microscopy, $n = 3$. In the I/R group, the mitochondria were enlarged, the cristae were ruptured, and the vacuoles were increased.

(B and E) Immunofluorescent staining of rat heart tissue with anti-TOMM20 antibody, observed under a fluorescence microscope, $n = 3$.

(C) Representative images of rat myocardial TUNEL staining, red fluorescent spots represent apoptotic cells, green fluorescent represent WGA, $n = 3$.

(F) Quantification of TUNEL fluorescent staining results, $n = 3$. (G) Determination of tissue ATP content, $n = 8$.

(H) Determination of tissue MDA level, $n = 8$. Experiments were repeated at least three times and the data are shown as mean ± SD. two-way ANOVA was used to compare differences. $^{*}p < 0.05$, $^{**}p < 0.01$, $^{***}p < 0.001$, $^{****}p < 0.0001$, ns represent not significant.

Corosolic acid induced prohibitin 2/PTEN-induced putative kinase protein-1/parkin-dependent mitophagy in the heart

Next, we tried to clarify the mechanism through which CA enhances mitochondrial structure and function. Mitophagy plays a protective role by removing damaged mitochondria.[40] Unfortunately, a complicated process occurs following cardiac I/R injury to impede mitophagy.[41] Interestingly, CA has been shown in studies to improve mitochondrial function.[42] Based on this, we discussed whether CA can trigger mitophagy to shield cardiomyocytes from I/R harm. The electron microscope image indicated that in comparison to the sham group, the mitochondria wrapped by autophagosome decreased in the I/R group, while the mitochondria wrapped by autophagosome increased markedly in the CA group. This is similar to the alleviative function of CA on myocardial I/R damage (Figure 3A).

According to a western blotting examination of mitophagy markers, rats treated with I/R had lower levels of PINK1 and Parkin in mitochondria of cardiac tissue, but rats treated with CA had higher levels of PINK1 and Parkin after I/R damage. Consistent with this, the expression of LC3B displayed dramatically down-regulated in the myocardial tissue of I/R rats. Rats receiving CA therapy showed increased LC3B. Additionally, PHB2 levels significantly decreased after I/R injury in mitochondria, but they returned to normal after CA therapy (Figures 3B and 3C). According to these findings, CA caused mitophagy via the PINK1/Parkin/PHB2 pathway.

CA protected H/R-injured cardiomyocytes and enhanced the expression of PHB2

To find the ideal concentration for an *in vitro* test, we examined the impact of various CA concentrations on cardiomyocyte viability with or without H/R. The cell survival of cardiomyocytes without H/R injury was unaffected by 5–20 μg/mL of CA (Figure 4A). Contrarily, H/R-damaged cardiomyocytes treated with 5–20 μg/mL of CA showed observably improved viability, and CA treatment inhibited LDH release (Figures 4B and 4C). Therefore, for subsequent tests, 10 μg/mL and 15 μg/mL CA was used. Damage to H/R causes cardiomyocytes to produce excessive amounts of reactive ROS.[43] Therefore, the level of ROS in cells can reflect the degree of cell damage. Immunofluorescence images made the reduction of ROS formation in hypoxia-reoxygenated H9C2 cells more visually (Figures 4D and 4E).

Next, we concentrated on the expression of proteins connected to mitophagy. Western blotting analysis displayed that the expression of PINK1, Parkin, and LC3B reduced, indicating that H/R suppressed the PINK1/Parkin-related mitophagy. These outcomes were altered by CA therapy. Additionally, CA treatment boosted PHB2 expression, which is downregulated during H/R (Figures 4F and 4G). According to these findings, CA controlled mitophagy linked to PINK1/Parkin and shielded cardiomyocytes from H/R damage.

Corosolic acid alleviates hypoxia/reoxygenation-induced mitochondrial dysfunction of myocardial cells

H/R-induced cardiomyocyte injury has been linked to mitochondrial damage, according to reports. We performed an electron microscope to observe mitochondrial structure, which demonstrated that H/R injury contributed to mitochondrial swelling with sparse cristae and empty vacuoles. CA treatment reduced the number and extent of damaged mitochondria in NRVMs (Figures 5A and 5D).

We employed JC-1 staining to find out how CA affected mitochondrial membrane potential, which is a crucial determinant of mitochondrial function. Red fluorescence signifies the polymer, and green fluorescence signifies the monomer. A lower polymer/monomer ratio showed that H/R caused the depolarization of the mitochondrial membrane potential in NRVMs, but CA processing can reverse this change (Figures 5B and 5E). Additionally, the Mito-SOX fluorescence signal was reduced by CA according to the fluorescent staining results, which suggests that CA reduced the buildup of Mito-ROS in the H/R-treated NRVMs (Figures 5C and 5F). Mitochondria are the body's energy factories. Therefore, when they suffer damage, the amount of ATP in the cell changes. According to the results of the ATP test, CA therapy increased the level of ATP during H/R while H/R decreased its amount in the myocardial cells compared to the control group (Figure 5G). These consequences suggested that CA plays a significant part in preserving mitochondrial function and structure during H/R.

Corosolic acid regulated PTEN-induced putative kinase protein-1/parkin-dependent mitophagy through prohibitin 2

In order to determine the downstream target and binding mode of CA in myocardial reperfusion injury, we carried out molecular docking using AutoDock Vina1.1.2 and visualized the results using PyMOL2.3.0 and Discovery Studio 2019. The binding energy between Corosolic acid and PHB2 is −6.9 kcal/mol, which has high binding stability. The analysis of the interaction mode between Corosolic acid and PHB2 found that there are mainly hydrogen bonds and hydrophobic interactions between the two. They form hydrogen bonds with GLU-38 and ARG-71, and the lengths of the hydrogen bonds are 3.3 Å and 2.9 Å, respectively; they have hydrophobic interactions with PRO-78, ILE-80, and PHE-41 (Figure 6A). Furthermore, to further prove whether the regulatory effect of Corosolic acid on PINK1/Parkin-associated mitophagy is exerted through PHB2, we knocked down the expression of PHB2 using siRNA. According to the western blotting results, siPHB2 reduced PHB2

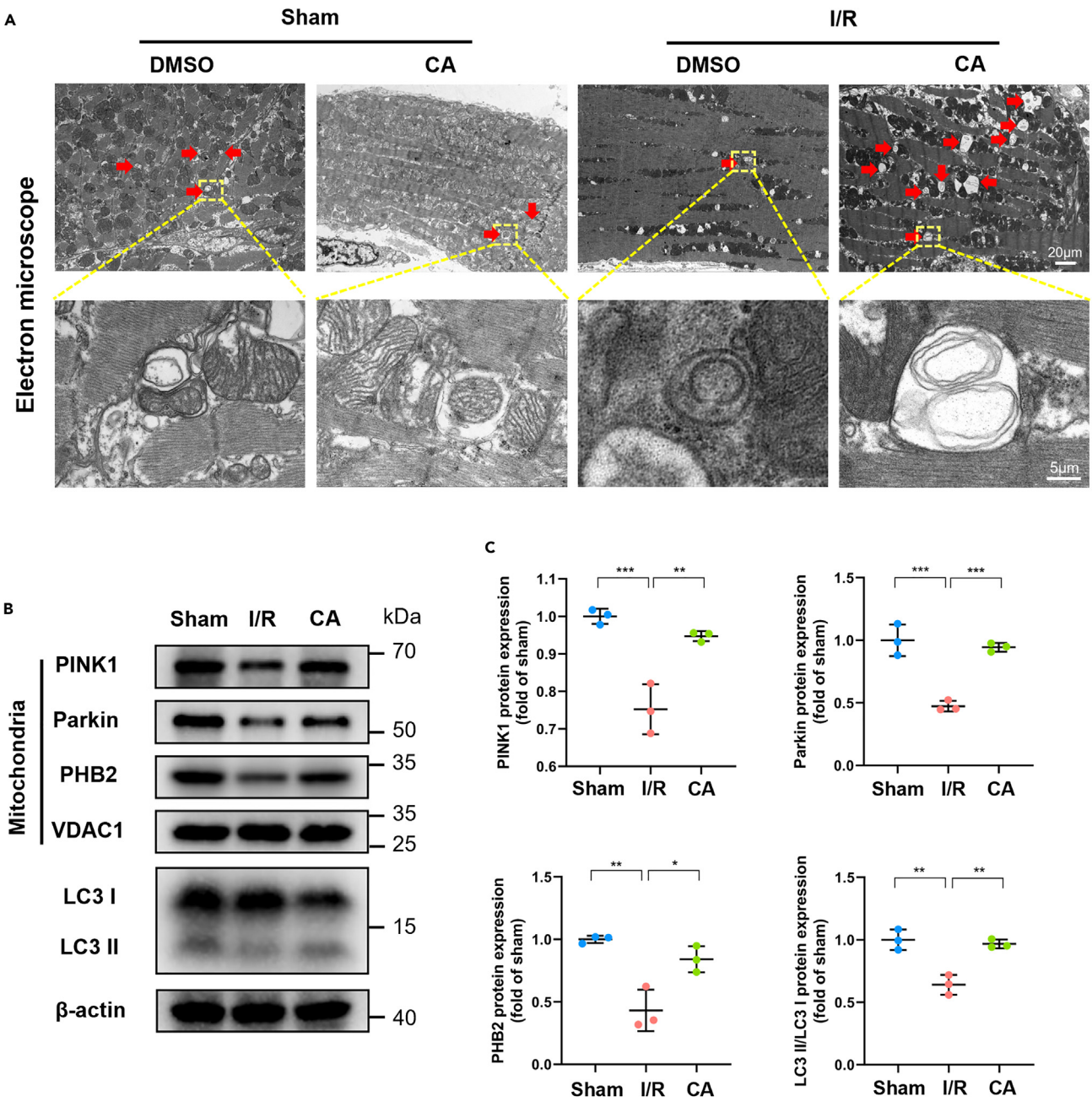

Figure 3. Corosolic acid increases mitophagy through the PHB2/PINK1/Parkin pathway

Rats were divided into a sham group and a myocardial I/R injury group with or without CA treatment.

(A) Transmission electron microscopy of reperfused cardiac myocardium, $n = 5$. Red arrows indicate mitochondria wrapped by autophagosomes.

(B and C) Presentative immunoblots and quantitative data of PHB2, PINK1, Parkin, and VDAC1 in the mitochondrial fractions and LC3B in heart tissue, $n = 3$. Experiments were repeated at least three times and the data are shown as mean ± SD. One-way ANOVA was used to compare differences. *$p < 0.05$, **$p < 0.01$, ***$p < 0.001$, ****$p < 0.0001$, ns represent not significant.

expression (Figure 6B). PHB2 knockdown appeared to block CA's effects on PINK1 and Parkin protein expression when compared to the CA group, indicating that CA controlled PINK1/Parkin through PHB2. PHB2 knockdown also eliminated CA's effects on the expression of the LC3B proteins, indicating that CA controlled mitophagy through PHB2 (Figures 6B and 6C). In addition, we used immunofluorescence co-localization to assess the extent of mitophagy. The red fluorescence represents mitochondria, and the green fluorescence is LC3B, which represents autophagosomes. The results demonstrated that siPHB2 decreased the increase in the co-localization of the mitochondria and

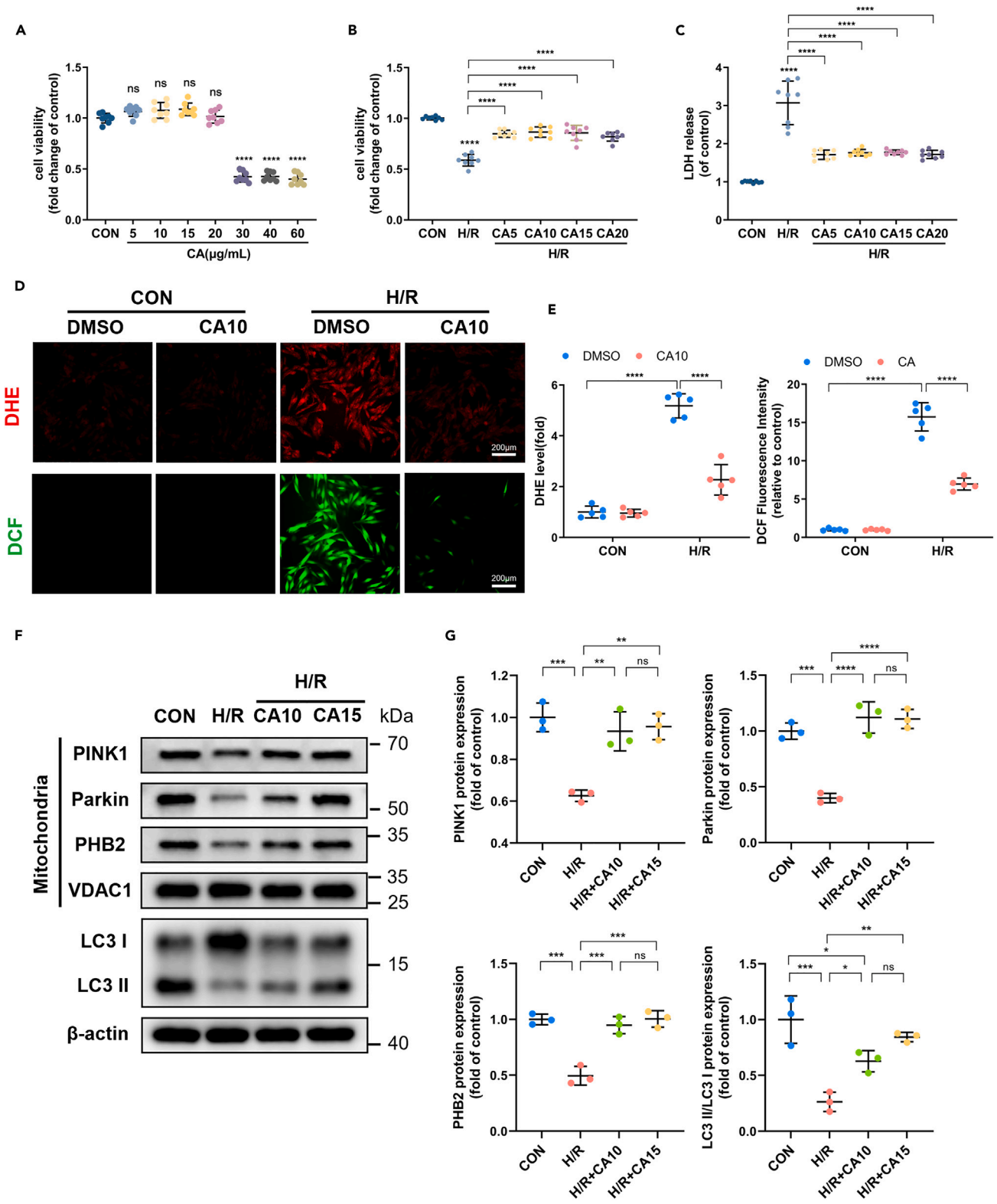

Figure 4. In cardiomyocytes, corosolic acid attenuates H/R-induced oxidative stress injury and enhances PINK1/Parkin-associated mitophagy

In vitro experiments, H9C2 cells were divided into the normal group and the H/R group. Different concentrations of corosolic acid were pretreated 24 h before H/R injury.

Figure 4. *Continued*

(A) The drug toxicity of corosolic acid at different concentrations (5, 10, 15, 20, 30, 40, 60 μg/mL) on H9C2 cells was detected under normoxia with CCK-8 detection kit, $n = 8$.

(B) The therapeutic effect of corosolic acid at different concentrations (5, 10, 15, 20 μg/mL) on H/R injury was detected by CCK-8 detection kit, $n = 8$.

(C) LDH of H/R injured H9C2 cell levels, $n = 8$.

(D and E) DHE and DCF levels of H9C2 cardiomyocytes detected by immunofluorescence microscopy. Red fluorescence is DHE staining and green fluorescence is DCF staining, $n = 5$.

(F and G) The expression of PHB2, PINK1, Parkin, and VDAC1 in mitochondria of H9C2 cells and the expression of LC3B in H9C2 cells, $n = 3$. Experiments were repeated at least three times and the data are shown as mean ± SD. (A, B, C, G) One-way ANOVA was used to compare differences. (E) two-way ANOVA was used to compare differences. $^{*}p < 0.05$, $^{**}p < 0.01$, $^{***}p < 0.001$, $^{****}p < 0.0001$, ns represent not significant.

autophagosomes generated by CA (Figure 6D). To further explore the colocalization of mitochondria and lysosomes, we used MitoTracker Green and LysoTracker red co-staining. As shown in the Figures S2B and S2C, mitochondria and lysosomes robustly co-localized within H/R treatment in CA-pretreated cells. However, mitochondria-lysosome associations were significantly reduced in similarly treated PHB2 deficient cells. These findings revealed that CA controlled PINK1/Parkin-dependent mitophagy through PHB2.

Prohibitin 2 was required for the mitochondrial protective effect of corosolic acid

Finally, we explored the protective capability of CA, and whether it depends on PHB2. We utilized siPHB2 to block the transcription of PHB2 in NRVMs and explored the mitochondrial protection provided by CA following H/R injury. We examined mitochondrial membrane potential, mitochondrial ROS, and ATP levels to evaluate the role of PHB2 in mitochondrial protection by CA. Results from JC-1 staining revealed that the CA group displayed considerably greater red fluorescence than the H/R group. However, CA + siPHB2 therapy reversed these modifications (Figures 7A, 7C, and 8). In addition, we isolated mitochondria in H9C2 cells for mitochondrial membrane potential detection. The results showed that PHB2 deletion significantly reduced mitochondrial membrane potential, which strongly supported that the protective effect of CA on mitochondria was partly through PHB2 (Figure S2E). Furthermore, the fluorescent staining results show that red fluorescence, which represents Mito-SOX, was observably reduced by CA treatment compared with the control group. However, siPHB2 is effective in eliminating the decreasing effect of CA on Mito-SOX (Figures 7B and 7D). Simultaneously, ATP content in the CA + siPHB2 group was considerably lower than that in the CA group during H/R (Figure 7E). We further investigated whether knocking down PHB2 would have an impact on mitochondrial function by measuring OCR. The results showed that PHB2 knockdown blocked the protective effect of CA on mitochondrial function (Figure S2D). Overall, this part of the study implies that CA improved mitochondrial function and oxidative stress partly depend on PHB2.

DISCUSSION

A prominent area of research in the realm of perioperative cardioprotection is cardiac I/R damage. There aren't many medications that can protect the heart from cardiac I/R injury since the molecular basis of I/R-induced myocardial damage is rather complex. In the current study, we revealed the PHB2/PINK1/Parkin mitophagy pathway's potential therapeutic utility for preserving the structure and functionality of cardiomyocytes during myocardial I/R injury. Additionally, we discovered that CA improved mitochondrial behavior by boosting mitophagy and preventing I/R-induced cardiomyocyte dysfunction. This is the first investigation, as far as we are aware, on the therapeutic ability of CA for cardiac I/R injury. Especially, these CA functions appeared to be dependent on mitophagy and the PHB2/PINK1/Parkin pathway, which protect mitochondria.

Cardiomyocytes require large amounts of energy to maintain cardiac contractile function. And under reperfusion conditions, mitochondrial-derived ROS production is increased, which in turn leads to lipid peroxidation, increased cell membrane permeability, and altered cytoarchitecture. Therefore, protection of cardiomyocyte mitochondria is critical to mitigate the damage caused by reperfusion. Previous studies have shown that the mitochondria-targeted S-nitrosothiol MitoSNO protects against I/R injury by inhibiting the reactivation of mitochondrial complex I during the first few minutes of reperfusion of ischemic tissue.[44] Malonate, a competitive succinate dehydrogenase inhibitor, effectively prevents succinate accumulation.[45] Malonate also prevents succinate maintaining a reduced CoQ pool and removes a driving force for RET to occur, preventing I/R injury by slowing succinate oxidation.[46] In addition, it has been reported that ischemic preconditioning (IPC) reduces the area of cardiac infarction after reperfusion. And mitochondria are the most important effector of IPC to exert its effect.[47] Although there are active preclinical studies that are constantly discovering new treatments for myocardial I/R injury, these approaches have not translated well into clinical practice.[48] Therefore, there is a need to discover new cardioprotective strategies with a view to their clinical application.

CA, an herbal extract, has multi-target and multi-pathway characteristics, stable efficacy, low toxicity, and promising clinical applications. In recent years, the role of CA in cardiomyocyte protection has been continuously explored. CA inhibited Dox-induced cardiotoxicity through AMP-activated protein kinase α2 (AMPKα2)/transcription factor EB (TFEB) mediated the restoration of autophagic flux and improvement of mitochondrial function.[39] Through regulating AMPK-dependent autophagy, CA exerted its cardiomyocyte protective benefits in a pressure overload-induced cardiac hypertrophy model.[37] CA demonstrated its protective effects in myocardial infarction mice by reducing oxidative stress, inflammation, and apoptosis to reduce heart fibrosis and dysfunction, which are linked to AMP-activated protein kinase (AMPK) activity.[49] Additional, CA also had defensive functions against non-alcoholic steatohepatitis brought on by a high-fat diet and carbon tetrachloride,[50] cerebral I/R injury, liver cancer, and colorectal cancer.[51–53] The studies revealed that CA has numerous biological impacts and merits

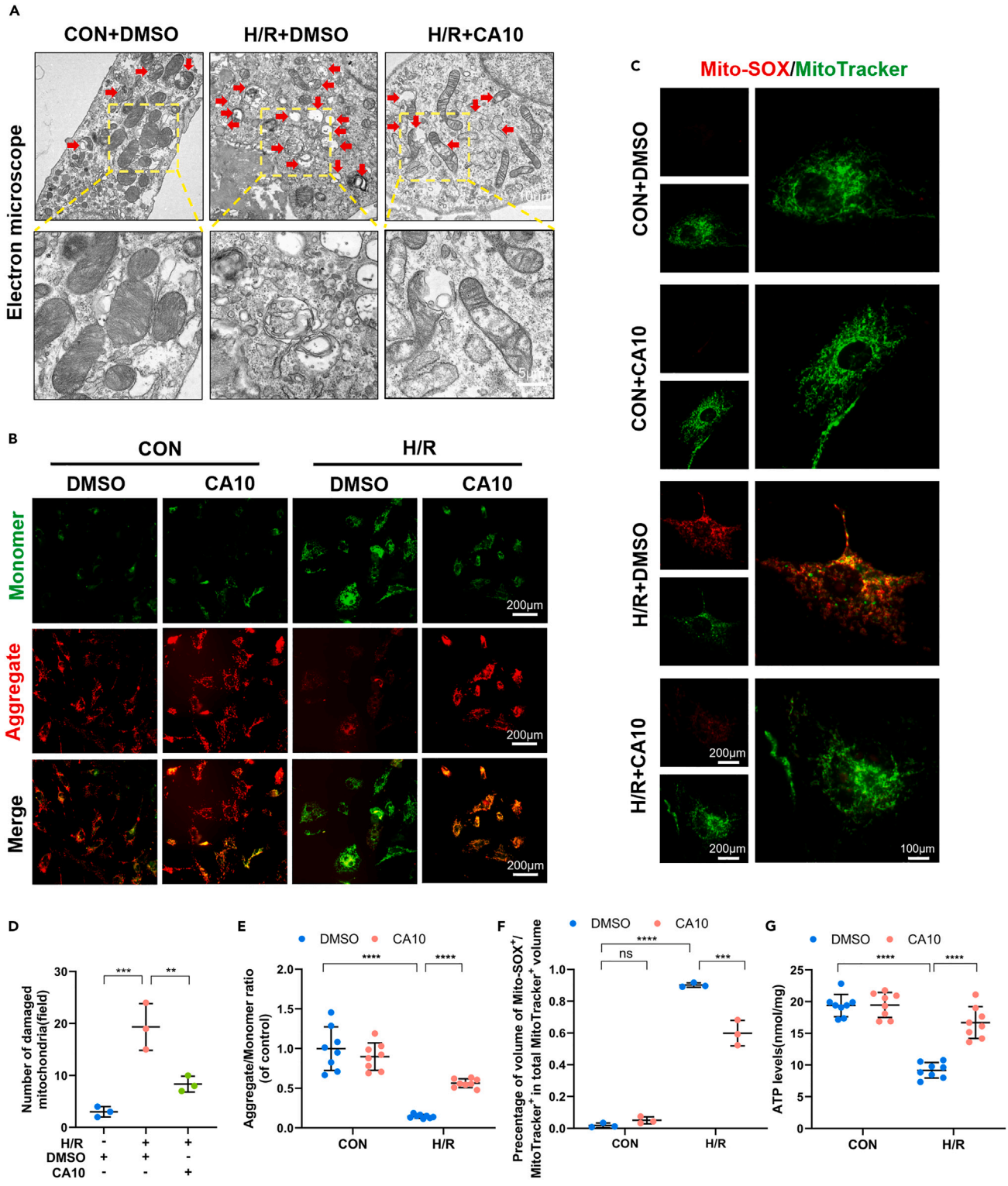

Figure 5. Corosolic acid alleviates mitochondrial dysfunction in cardiomyocytes induced by H/R injury

Cardiomyocytes were divided into the normal group and the H/R group. The treatment group was pretreated with corosolic acid (10 μg/mL) 24 h before H/R injury.

(A and D) The changes of mitochondria in H/R primary cardiomyocytes were observed by transmission electron microscopy, $n = 3$. In the H/R group, the mitochondria were enlarged, the cristae were ruptured, and the vacuoles were increased.

Figure 5. *Continued*

(B and E) Mitochondrial membrane potential of NRVMs was detected and quantified by immunofluorescence, $n = 8$.

(C and F) Representative images of Mito-SOX and MitoTracker-Green in NRVMs. Fraction of Mito-SOX that overlaps with MitoTracker-Green labeled mitochondria was quantified by Manders' colocalization coefficient, $n = 3$.

(G) ATP levels in cardiomyocytes, $n = 8$. Experiments were repeated at least three times and the data are shown as mean ± SD.

(D) One-way ANOVA was used to compare differences.

(E–G) two-way ANOVA was used to compare differences. *$p < 0.05$, **$p < 0.01$, ***$p < 0.001$, ****$p < 0.0001$, ns represent not significant.

further, in-depth investigation. We anticipated that CA had protective effects against heart harm caused by I/R in light of the cardiomyocyte protection it provided in other studies. In this work, CA prevented apoptosis, decreased oxidative stress, and protected the heart from I/R-induced histopathological injury. It also enhanced heart function, as seen by higher levels of LVEF% and LVFS%. These findings validated the role of CA in preventing cardiac damage brought on by I/R. The potential mechanism to explain these effects was also looked into.

Our animal experiments showed that CA improves the structure and function of the heart after reperfused myocardial infarction, and reduces apoptosis as well as mitochondrial function damage. In order to better control the experimental conditions and avoid confounding the effects of circulating factors, such as hormones, neurotransmitters, and cytokines, we performed *in vitro* experiments. Cardiomyocytes (~50%) represent the largest proportion of ventricular cells with the highest mitochondrial content (~30%).[54] This means that cardiomyocytes play a very important role in maintaining heart function. But that the isolated cardiomyocyte culture approach only targets these and no other cell types, which can be an advantage but also a disadvantage. Freshly isolated cardiomyocytes eliminate potential confounding factors for phenotypic transformation in culture and are a better choice for *in vitro* experiments.[55] Freshly isolated cardiomyocytes include freshly isolated adult rat cardiomyocytes and NRVMs. Although freshly isolated adult rat cardiomyocytes are more consistent with the clinical situation that ischemic heart disease occurs almost exclusively in adults, adult rat cardiomyocytes are difficult to isolate and do not survive long in cell culture.[55] Whereas in our study the cells were subjected to drug pretreatment, H/R, and transfection for a longer time span. Therefore, NRVMs that are relatively easy to isolate and survive for a longer period of time are a better choice for us in this case. In addition, in the mechanism study part, we chose another commonly used cell in H/R experiments, H9C2 cells,[55] which are a cell line cloned from rat cardiomyocytes. H9C2 cells are convenient to obtain in large quantities, which facilitates the exploration of the mechanism. Experiments using both NRVM and H9C2 cells can complement each other's strengths and show the accuracy of the experiments in a more comprehensive way.

Anaerobic glycolysis and the accumulation of acidic metabolites brought on by cardiac I/R damage compromise mitochondrial activity and cause the loss of dynamic homeostasis in the mitochondria. Energy metabolism's primary byproduct is ROS, which is mostly created by mitochondria and removed by mitochondrial antioxidant proteins. When mitochondria are dysfunctional or ROS are overproduced, redox is out of balance, and the excess ROS, in turn, can further aggravate mitochondrial damage. In our investigation, we found that the I/R group had an accumulation of ROS and MDA, as well as more swollen mitochondria. The findings also suggested that I/R caused a metabolic malfunction in the heart's mitochondria, which was supported by an accumulation of Mito-SOX and a diminishment of ATP contents. By correcting these modifications, CA therapy enhanced mitochondrial function.

Mitophagy, which uses the lysosomal pathway to remove damaged or old mitochondria, is crucial for preserving mitochondrial homeostasis.[56] However, mitophagy is largely blocked during prolonged ischemia and subsequent reperfusion as a result of a number of processes.[23,41,57] Interestingly, we discovered that CA reduced rat mitochondrial damage by restoring mitophagy during I/R injury via starting the PHB2/PINK1/Parkin pathway. However, when PHB2 was knocked out, CA failed to increase PINK1/Parkin-associated mitophagy and alleviate mitochondrial damage. These results showed that CA largely preserved mitophagy under I/R injury to sustain myocardial mitochondrial performance.

One of the most significant mitophagy processes, PINK1/Parkin-mediated mitophagy, is involved in the removal of defective mitochondria after cardiac I/R-induced damage.[58] Under normal circumstances, Parkin adopts an autoinhibited shape, and the cytosolic ligase is deactivated.[59] Following the depolarization of the mitochondria, PINK1 builds up at the inner membrane, where it attracts Parkin from the cytoplasm and turns on E3 ligase activity. Parkin then ubiquitinates a number of outer membrane proteins to trigger the onset of mitophagy.[60] PHB2, an inner mitochondrial membrane protein, is involved in targeted mitochondrial autophagy degradation.[32] Depletion of PHB2 destabilizes PINK1 in the mitochondria, which prevents PRKN/Parkin and ubiquitin from being recruited to the mitochondria after the depolarization of the mitochondrial membrane or the aggregation of misfolded proteins and inhibits mitophagy.[33] The significance of PHB2/PINK1/Parkin-mediated mitophagy in CA-induced cardiomyocyte protection is not well clear.

Our current research manifested that CA activated PHB2 to induce PINK1/Parkin-dependent mitophagy (Figure 8). This is the first proof that CA and the PHB2/PINK1/Parkin mitophagy pathway are connected. Our *in vitro* genetic knock-down experiments and biochemical analyses unequivocally demonstrated that this pathway enhanced mitochondrial integrity and cardiac cell function. Thus, the PHB2/PINK1/Parkin mitophagy pathway may be a crucial coordinator of the response to CA in the pathophysiology of heart I/R damage.

Limitations of the study

The current study has a number of flaws. First, although we achieved PHB2 knockdown using siPHB2 *in vitro* experiments and investigated the corresponding mechanism, *in vivo* experimental evidence is lacking. Second, even though we described how PHB2 affected PINK1/Parkin-related mitophagy in I/R-induced cardiac damage, more investigation is still required to pinpoint the specific regulatory mechanism between PHB2 and PINK1/Parkin.

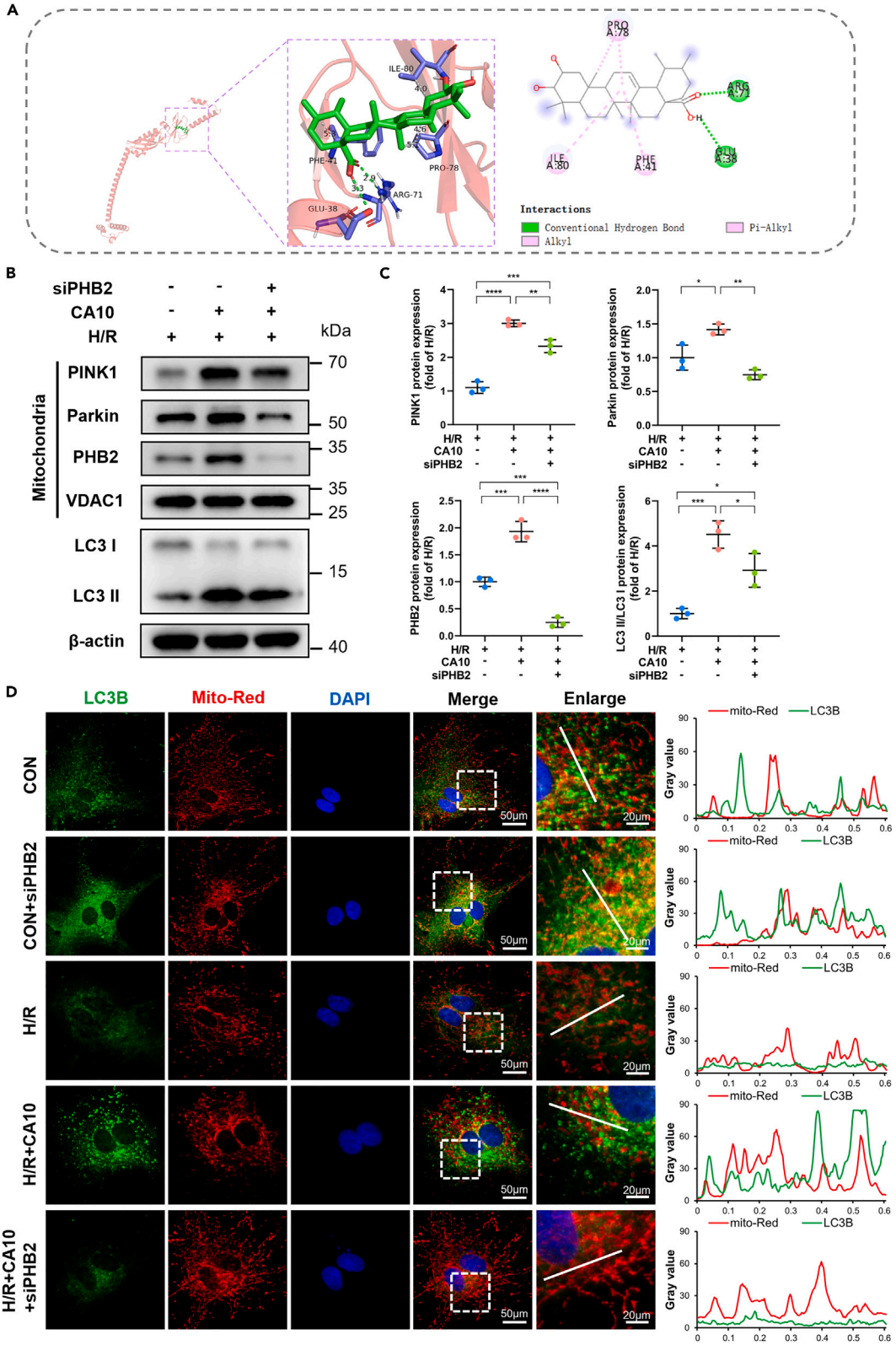
A
ILE-80
PHE-41
PRO-78
ARG-71
GLU-38
PRO A:78
ARG A:71
ILE A:80
PHE A:41
GLU A:38
Interactions
Conventional Hydrogen Bond
Pi-Alkyl
Alkyl
B
siPHB2
CA10
H/R
kDa
Mitochondria
PINK1
Parkin
PHB2
VDAC1
LC3 I
LC3 II
β-actin
70
50
35
35
25
15
40
C
PINK1 protein expression (fold of H/R)
Parkin protein expression (fold of H/R)
PHB2 protein expression (fold of H/R)
LC3 II/LC3 I protein expression (fold of H/R)
H/R
CA10
siPHB2
D
LC3B
Mito-Red
DAPI
Merge
Enlarge
CON
CON+siPHB2
H/R
H/R+CA10
H/R+CA10 +siPHB2
50μm
20μm
mito-Red
LC3B
Gray value

Figure 6. Knockdown of PHB2 prevents the corosolic acid regulation of PINK1/Parkin-associated mitophagy in H/R cardiomyocytes

The siPHB2 cardiomyocytes were divided into the normal group and the H/R group. The treatment group was pretreated with corosolic acid (10 μg/mL) 24 h before H/R injury.

(A) Interaction mode analysis of corosolic acid and PHB2 protein using PyMOL2.3.0 and Discovery Studio 2019.

(B and C) H9C2 cells were treated with CA at 10 μg/mL and mitochondrial fractions were isolated for western blotting analysis of PHB2, PINK1, Parkin, and VDAC1, and LC3B was detected in H9C2 cells, $n = 3$.

(D) Mitochondria were stained red (mito-Red) with a mitochondria-specific dye, followed by immunofluorescent staining with an anti-LC3B antibody. DAPI stains nuclei. Observe under a fluorescence microscope. The line chart on the right shows the pixel intensity of mito-Red and LC3B on one line. Experiments were repeated at least three times and the data are shown as mean ± SD. One-way ANOVA was used to compare differences. *$p < 0.05$, **$p < 0.01$, ***$p < 0.001$, ****$p < 0.0001$, ns represent not significant.

STAR★METHODS

Detailed methods are provided in the online version of this paper and include the following:

- KEY RESOURCES TABLE
- RESOURCE AVAILABILITY
  - Lead contact
  - Materials availability
  - Data and code availability
- EXPERIMENTAL MODEL AND STUDY PARTICIPANT DETAILS
  - Animals
- METHOD DETAILS
  - Rat model of myocardial I/R injury
  - TTC and Evans blue staining
  - Transthoracic echocardiography
  - Transmission electron microscopy
  - Hematoxylin and Eosin (H&E) staining
  - Immunofluorescence and immunohistochemistry
  - CCK-8 and LDH
  - Quantification of ATP and MDA
  - Serum levels of BNP and cTnT
  - TUNEL staining
  - Cell culture and treatment
  - Small interfering RNA (siRNA) transfection
  - Mitochondrial isolation
  - Western blotting
  - ROS staining and mitochondrial membrane potential measurement
  - Measurement of oxygen consumption rate (OCR)
  - Molecular docking
  - Statistical analysis

SUPPLEMENTAL INFORMATION

Supplemental information can be found online at https://doi.org/10.1016/j.isci.2024.110448.

ACKNOWLEDGMENTS

This study was supported by grants from the National Natural Science Foundation of China (Nos.81770327 and 81100173), the Natural Science Foundation of Jiangsu Province (Grant No. BK20231198), and Jiangsu Province Health Care Development Special Fund (M2022038, China). BioRender was used to generate schematic figures.

AUTHOR CONTRIBUTIONS

HXL, TBJ, and JZ designed the experiments. TKY, MYT, and JZ performed the experiments. YJZ, LY, YFJ, LHH, and XM performed some of the experiments. JZ, YML, and YFY wrote the article. All authors read and approved the final article.

DECLARATION OF INTERESTS

No potential conflict of interest was reported by the authors.

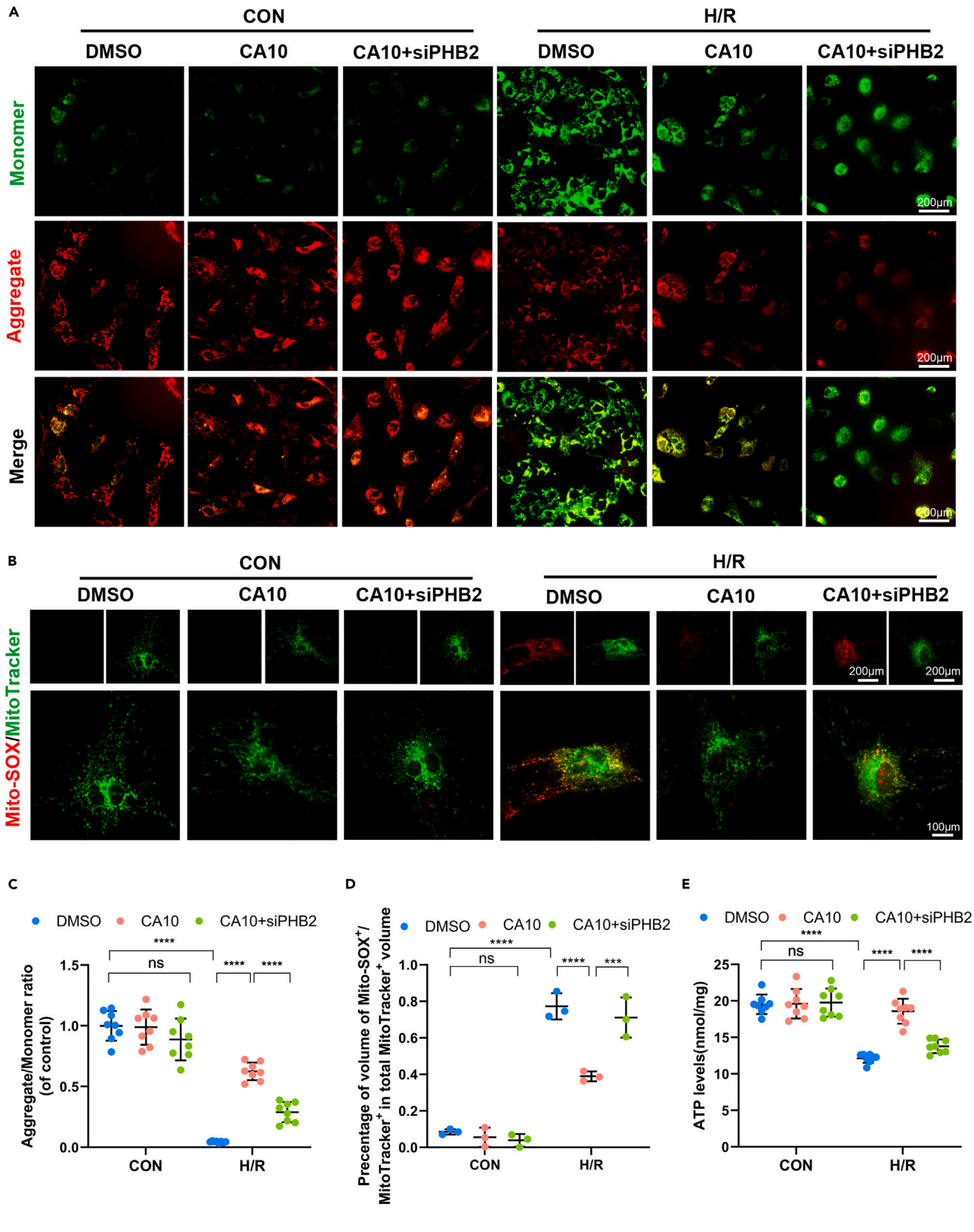
A
CON
H/R
DMSO
CA10
CA10+siPHB2
DMSO
CA10
CA10+siPHB2
Monomer
Aggregate
Merge
200μm
200μm
200μm
B
CON
H/R
DMSO
CA10
CA10+siPHB2
DMSO
CA10
CA10+siPHB2
Mito-SOX/MitoTracker
200μm
200μm
100μm
C
DMSO
CA10
CA10+siPHB2
Aggregate/Monomer ratio (of control)
1.5
1.0
0.5
0.0
****
ns
****
****
CON
H/R
D
DMSO
CA10
CA10+siPHB2
Precentage of volume of Mito-SOX+/ MitoTracker+ in total MitoTracker+ volume
1.0
0.8
0.6
0.4
0.2
0.0
****
ns
****
***
CON
H/R
E
DMSO
CA10
CA10+siPHB2
ATP levels(nmol/mg)
25
20
15
10
5
0
****
ns
****
****
CON
H/R

Figure 7. Knockdown of PHB2 prevented the protective action of corosolic acid on mitochondria in H/R NRVMs

The siPHB2 cardiomyocytes were divided into the normal group and the H/R group. The treatment group was pretreated with corosolic acid (10 μg/mL) 24 h before H/R injury.

(A and C) Immunofluorescence detection of mitochondrial membrane potential in NRVMs, $n = 8$.

(B and D) Representative images of Mito-SOX and MitoTracker-Green in NRVMs. Fraction of Mito-SOX that overlaps with MitoTracker-Green labeled mitochondria was quantified by Manders' colocalization coefficient, $n = 3$.

(E) ATP levels in NRVMs, $n = 8$. Experiments were repeated at least three times and the data are shown as mean ± SD. two-way ANOVA was used to compare differences. *$p < 0.05$, **$p < 0.01$, ***$p < 0.001$, ****$p < 0.0001$, ns represent not significant.

Received: October 12, 2023
Revised: January 20, 2024
Accepted: July 1, 2024
Published: July 8, 2024

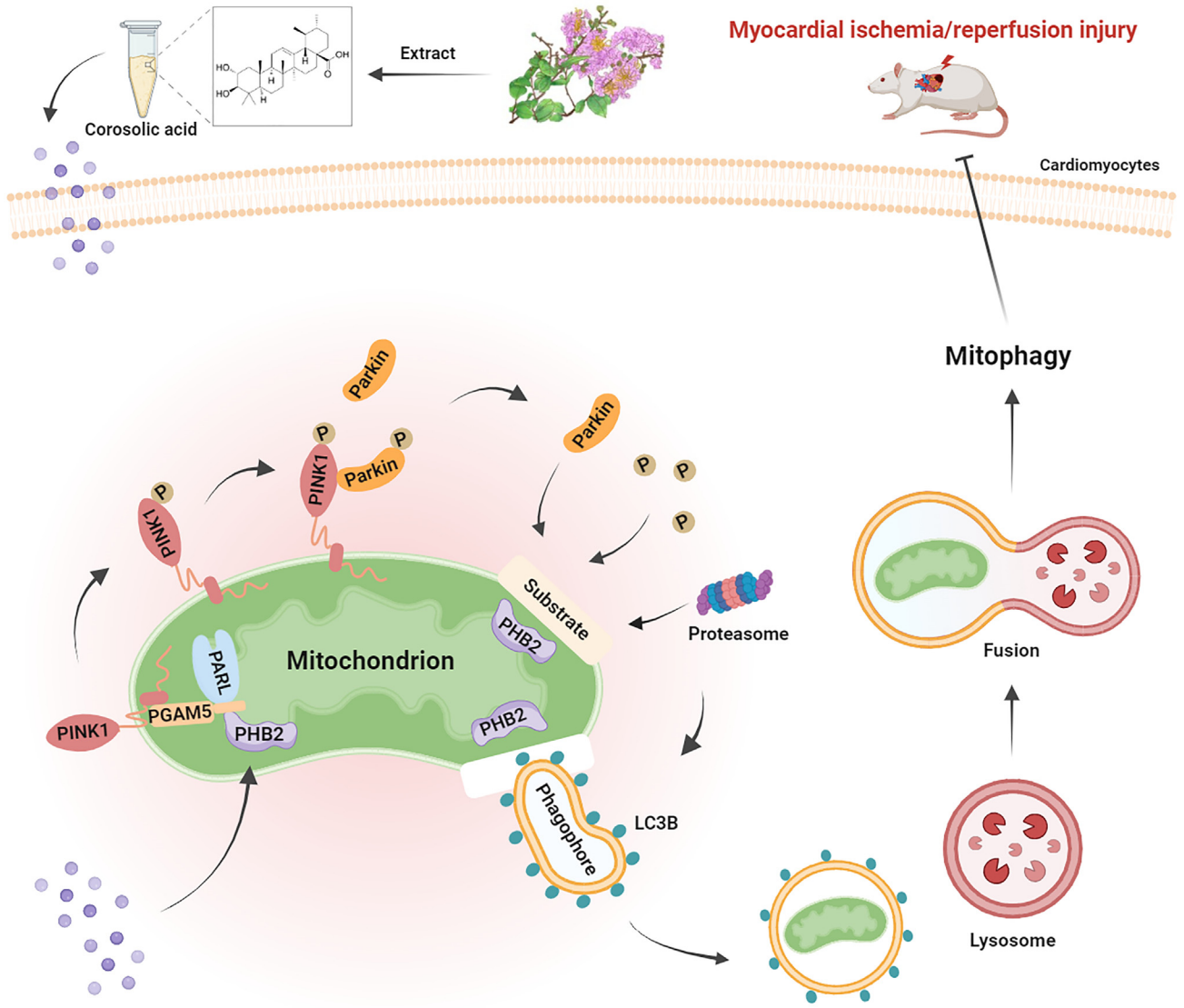

Figure 8. In cardiomyocytes, corosolic acid regulates the mode of action on the PHB2/PINK1/Parkin/mitophagy pathway

Corosolic acid can increase PHB2 in myocardial I/R injury. PHB2 binds to PARL to prevent PGAM5 from being cleaved. Full-length PGAM5 protects PINK1 from translocating to the mitochondrial outer membrane rather than being cleaved. Full-length PINK1 recruits Parkin to mitochondria. The mitochondrial outer membrane is subsequently ubiquitinated and degraded by the proteasome. Subsequently, PHB2 located in the inner mitochondrial membrane is recognized by LC3B on the autophagosome to initiate mitophagy. PARL: presenilin associated rhomboid like, PGAM5: PGAM family member 5, mitochondrial serine/threonine protein phosphatase.

REFERENCES

1. Zhou, H., Ma, Q., Zhu, P., Ren, J., Reiter, R.J., and Chen, Y. (2018). Protective role of melatonin in cardiac ischemia-reperfusion injury: From pathogenesis to targeted therapy. J. Pineal Res. *64*, e12471.
2. (2020). Global burden of 369 diseases and injuries in 204 countries and territories, 1990-2019: a systematic analysis for the Global Burden of Disease Study 2019. Lancet *396*, 1204–1222.
3. Kakavand, H., Aghakouchakzadeh, M., Coons, J.C., and Talasaz, A.H. (2021). Pharmacologic Prevention of Myocardial Ischemia-Reperfusion Injury in Patients With Acute Coronary Syndrome Undergoing Percutaneous Coronary Intervention. J. Cardiovasc. Pharmacol. *77*, 430–449.
4. Jovancevic, N., Dendorfer, A., Matzkies, M., Kovarova, M., Heckmann, J.C., Osterloh, M., Boehm, M., Weber, L., Nguemo, F., Semmler, J., et al. (2017). Medium-chain fatty acids modulate myocardial function via a cardiac odorant receptor. Basic Res. Cardiol. *112*, 13.
5. Zhai, M., Li, B., Duan, W., Jing, L., Zhang, B., Zhang, M., Yu, L., Liu, Z., Yu, B., Ren, K., et al. (2017). Melatonin ameliorates myocardial ischemia reperfusion injury through SIRT3-dependent regulation of oxidative stress and apoptosis. J. Pineal Res. *63*, e12419.
6. Khan, H., Gupta, A., Singh, T.G., and Kaur, A. (2021). Mechanistic insight on the role of leukotriene receptors in ischemic-reperfusion injury. Pharmacol. Rep. *73*, 1240–1254.
7. Hajjar, D.P., and Gotto, A.M. (2013). Biological relevance of inflammation and oxidative stress in the pathogenesis of arterial diseases. Am. J. Pathol. *182*, 1474–1481.
8. Picca, A., Mankowski, R.T., Burman, J.L., Donisi, L., Kim, J.-S., Marzetti, E., and Leeuwenburgh, C. (2018). Mitochondrial quality control mechanisms as molecular targets in cardiac ageing. Nat. Rev. Cardiol. *15*, 543–554.
9. Chang, X., Lochner, A., Wang, H.-H., Wang, S., Zhu, H., Ren, J., and Zhou, H. (2021). Coronary microvascular injury in myocardial infarction: perception and knowledge for mitochondrial quality control. Theranostics *11*, 6766–6785.
10. Marin, W., Marin, D., Ao, X., and Liu, Y. (2021). Mitochondria as a therapeutic target for cardiac ischemia-reperfusion injury (Review). Int. J. Mol. Med. *47*, 485–499.
11. Wang, J., and Zhou, H. (2020). Mitochondrial quality control mechanisms as molecular targets in cardiac ischemia-reperfusion injury. Acta Pharm. Sin. B *10*, 1866–1879.
12. Tan, Y., Mui, D., Toan, S., Zhu, P., Li, R., and Zhou, H. (2020). SERCA Overexpression Improves Mitochondrial Quality Control and Attenuates Cardiac Microvascular Ischemia-Reperfusion Injury. Mol. Ther. Nucleic Acids *22*, 696–707.
13. Ramachandra, C.J.A., Hernandez-Resendiz, S., Crespo-Avilan, G.E., Lin, Y.-H., and Hausenloy, D.J. (2020). Mitochondria in acute myocardial infarction and cardioprotection. EBioMedicine *57*, 102884.
14. Fuhrmann, D.C., and Brüne, B. (2017). Mitochondrial composition and function under the control of hypoxia. Redox Biol. *12*, 208–215.
15. Xu, J., Wu, Y., Lu, G., Xie, S., Ma, Z., Chen, Z., Shen, H.-M., and Xia, D. (2017). Importance of ROS-mediated autophagy in determining apoptotic cell death induced by physapubescin B. Redox Biol. *12*, 198–207.
16. He, S., Wang, X., and Chen, A. (2017). Myocardial ischemia/reperfusion injury: the role of adaptor proteins Crk. Perfusion *32*, 345–349.
17. Mui, D., and Zhang, Y. (2021). Mitochondrial scenario: roles of mitochondrial dynamics in acute myocardial ischemia/reperfusion injury. J. Recept. Signal Transduct. Res. *41*, 1–5.
18. Wang, J., Toan, S., and Zhou, H. (2020). Mitochondrial quality control in cardiac microvascular ischemia-reperfusion injury: New insights into the mechanisms and therapeutic potentials. Pharmacol. Res. *156*, 104771.
19. Gao, X., Li, H., Zhang, W., Wang, X., Sun, H., Cao, Y., Zhao, Y., Ji, H., Yang, F., Ma, W., et al. (2022). Photobiomodulation Drives MiR-136-5p Expression to Promote Injury Repair after Myocardial Infarction. Int. J. Biol. Sci. *18*, 2980–2993.
20. Huang, J., Li, R., and Wang, C. (2021). The Role of Mitochondrial Quality Control in Cardiac Ischemia/Reperfusion Injury. Oxid. Med. Cell. Longev. *2021*, 5543452.
21. Buja, L.M. (2005). Myocardial ischemia and reperfusion injury. Cardiovasc. Pathol. *14*, 170–175.
22. Wang, S., Wang, Y., Cheng, H., Zhang, Q., Fu, C., He, C., and Wei, Q. (2022). The Networks of Noncoding RNAs and Their Direct Molecular Targets in Myocardial Infarction. Int. J. Biol. Sci. *18*, 3194–3208.
23. Zhou, H., Zhu, P., Wang, J., Zhu, H., Ren, J., and Chen, Y. (2018). Pathogenesis of cardiac ischemia reperfusion injury is associated with CK2α-disturbed mitochondrial homeostasis via suppression of FUNDC1-related mitophagy. Cell Death Differ. *25*, 1080–1093.
24. Titus, A.S., Sung, E.A., Zablocki, D., and Sadoshima, J. (2023). Mitophagy for cardioprotection. Basic Res. Cardiol. *118*, 42.
25. Tu, M., Tan, V.P., Yu, J.D., Tripathi, R., Bigham, Z., Barlow, M., Smith, J.M., Brown, J.H., and Miyamoto, S. (2022). RhoA signaling increases mitophagy and protects cardiomyocytes against ischemia by stabilizing PINK1 protein and recruiting Parkin to mitochondria. Cell Death Differ. *29*, 2472–2486.
26. Wu, L., Wang, L., Du, Y., Zhang, Y., and Ren, J. (2023). Mitochondrial quality control mechanisms as therapeutic targets in doxorubicin-induced cardiotoxicity. Trends Pharmacol. Sci. *44*, 34–49.
27. Tong, M., Saito, T., Zhai, P., Oka, S.-I., Mizushima, W., Nakamura, M., Ikeda, S., Shirakabe, A., and Sadoshima, J. (2019). Mitophagy Is Essential for Maintaining Cardiac Function During High Fat Diet-Induced Diabetic Cardiomyopathy. Circ. Res. *124*, 1360–1371.
28. Turkieh, A., El Masri, Y., Pinet, F., and Dubois-Deruy, E. (2022). Mitophagy Regulation Following Myocardial Infarction. Cells *11*, 199.
29. Sekine, S., and Youle, R.J. (2018). PINK1 import regulation; a fine system to convey mitochondrial stress to the cytosol. BMC Biol. *16*, 2.
30. Xiong, W., Hua, J., Liu, Z., Cai, W., Bai, Y., Zhan, Q., Lai, W., Zeng, Q., Ren, H., and Xu, D. (2018). PTEN induced putative kinase 1 (PINK1) alleviates angiotensin II-induced cardiac injury by ameliorating mitochondrial dysfunction. Int. J. Cardiol. *266*, 198–205.
31. Soh, J.E.C., Shimizu, A., Molla, M.R., Zankov, D.P., Nguyen, L.K.C., Khan, M.R., Tesega, W.W., Chen, S., Tojo, M., Ito, Y., et al. (2023). RhoA rescues cardiac senescence by regulating Parkin-mediated mitophagy. J. Biol. Chem. *299*, 102993.
32. Wei, Y., Chiang, W.-C., Sumpter, R., Mishra, P., and Levine, B. (2017). Prohibitin 2 Is an Inner Mitochondrial Membrane Mitophagy Receptor. Cell *168*, 224–238.e10.
33. Yan, C., Gong, L., Chen, L., Xu, M., Abou-Hamdan, H., Tang, M., Désaubry, L., and Song, Z. (2020). PHB2 (prohibitin 2) promotes PINK1-PRKN/Parkin-dependent mitophagy by the PARL-PGAM5-PINK1 axis. Autophagy *16*, 419–434.
34. Wang, K., Long, B., Zhou, L.-Y., Liu, F., Zhou, Q.-Y., Liu, C.-Y., Fan, Y.-Y., and Li, P.-F. (2014). CARL lncRNA inhibits anoxia-induced mitochondrial fission and apoptosis in cardiomyocytes by impairing miR-539-dependent PHB2 downregulation. Nat. Commun. *5*, 3596.
35. Jin, M., Wu, Y., Lou, Y., Liu, X., Dai, Y., Yang, W., Liu, C., and Huang, G. (2021). Corosolic acid reduces A549 and PC9 cell proliferation, invasion, and chemoresistance in NSCLC via inducing mitochondrial and liposomal oxidative stress. Biomed. Pharmacother. *144*, 112313.
36. Zhang, C., Niu, Y., Wang, Z., Xu, X., Li, Y., Ma, L., Wang, J., and Yu, Y. (2021). Corosolic acid inhibits cancer progression by decreasing the level of CDK19-mediated O-GlcNAcylation in liver cancer cells. Cell Death Dis. *12*, 889.
37. Wang, Z.-P., Shen, D., Che, Y., Jin, Y.-G., Wang, S.-S., Wu, Q.-Q., Zhou, H., Meng, Y.-Y., and Yuan, Y. (2019). Corosolic acid ameliorates cardiac hypertrophy via regulating autophagy. Biosci. Rep. *39*, BSR20191860.
38. Alkholifi, F.K., Devi, S., Yusufoglu, H.S., and Alam, A. (2023). The Cardioprotective Effect of Corosolic Acid in the Diabetic Rats: A Possible Mechanism of the PPAR-γ Pathway. Molecules *28*, 929.
39. Che, Y., Wang, Z., Yuan, Y., Zhou, H., Wu, H., Wang, S., and Tang, Q. (2022). By restoring autophagic flux and improving mitochondrial function, corosolic acid protects against Dox-induced cardiotoxicity. Cell Biol. Toxicol. *38*, 451–467.
40. Tripathi, A., Scaini, G., Barichello, T., Quevedo, J., and Pillai, A. (2021). Mitophagy in depression: Pathophysiology and treatment targets. Mitochondrion *61*, 1–10.
41. Wu, H., Ye, M., Liu, D., Yang, J., Ding, J.-W., Zhang, J., Wang, X.-A., Dong, W.-S., Fan, Z.-X., and Yang, J. (2019). UCP2 protect the heart from myocardial ischemia/reperfusion injury via induction of mitochondrial autophagy. J. Cell. Biochem. *120*, 15455–15466.
42. Yamaguchi, Y., Yamada, K., Yoshikawa, N., Nakamura, K., Haginaka, J., and Kunitomo, M. (2006). Corosolic acid prevents oxidative stress, inflammation and hypertension in SHR/NDmcr-cp rats, a model of metabolic syndrome. Life Sci. *79*, 2474–2479.
43. Wang, L., Qiu, S., Li, X., Zhang, Y., Huo, M., and Shi, J. (2023). Myocardial-Targeting Tannic Cerium Nanocatalyst Attenuates Ischemia/Reperfusion Injury. Angew. Chem. Int. Ed. Engl. *62*, e202305576.
44. Methner, C., Chouchani, E.T., Buonincontri, G., Pell, V.R., Sawiak, S.J., Murphy, M.P., and Krieg, T. (2014). Mitochondria selective

S-nitrosation by mitochondria-targeted S-nitrosothiol protects against post-infarct heart failure in mouse hearts. Eur. J. Heart Fail. *16*, 712–717.

45. Kula-Alwar, D., Prag, H.A., and Krieg, T. (2019). Targeting Succinate Metabolism in Ischemia/Reperfusion Injury. Circulation *140*, 1968–1970.
46. Chouchani, E.T., Pell, V.R., Gaude, E., Aksentijević, D., Sundier, S.Y., Robb, E.L., Logan, A., Nadtochiy, S.M., Ord, E.N.J., Smith, A.C., et al. (2014). Ischaemic accumulation of succinate controls reperfusion injury through mitochondrial ROS. Nature *515*, 431–435.
47. Heusch, G. (2015). Molecular basis of cardioprotection: signal transduction in ischemic pre-post-and remote conditioning. Circ. Res. *116*, 674–699.
48. Heusch, G. (2023). Cardioprotection and its Translation: A Need for New Paradigms? Or for New Pragmatism? An Opinionated Retro- and Perspective. J. Cardiovasc. Pharmacol. Ther. *28*, 10742484231179613.
49. Wang, Z.-P., Che, Y., Zhou, H., Meng, Y.-Y., Wu, H.-M., Jin, Y.-G., Wu, Q.-Q., Wang, S.-S., and Yuan, Y. (2020). Corosolic acid attenuates cardiac fibrosis following myocardial infarction in mice. Int. J. Mol. Med. *45*, 1425–1435.
50. Liu, G., Cui, Z., Gao, X., Liu, H., Wang, L., Gong, J., Wang, A., Zhang, J., Ma, Q., Huang, Y., et al. (2021). Corosolic acid ameliorates non-alcoholic steatohepatitis induced by high-fat diet and carbon tetrachloride by regulating TGF-β1/Smad2, NF-κB, and AMPK signaling pathways. Phytother Res. *35*, 5214–5226.
51. Zhang, B.-Y., Zhang, L., Chen, Y.-M., Qiao, X., Zhao, S.-L., Li, P., Liu, J.-F., Wen, X., and Yang, J. (2021). Corosolic acid inhibits colorectal cancer cells growth as a novel HER2/HER3 heterodimerization inhibitor. Br. J. Pharmacol. *178*, 1475–1491.
52. Peng, Y., Li, N., Tang, F., Qian, C., Jia, T., Liu, J., and Xu, Y. (2022). Corosolic acid sensitizes ferroptosis by upregulating HERPUD1 in liver cancer cells. Cell Death Discov. *8*, 376.
53. Zhang, L., Sui, S., Wang, S., and Sun, J. (2022). Neuroprotective Effect of Corosolic Acid Against Cerebral Ischemia-Reperfusion Injury in Experimental Rats. J. Oleo Sci. *71*, 1501–1510.
54. Litvinukova, M., Talavera-Lopez, C., Maatz, H., Reichart, D., Worth, C.L., Lindberg, E.L., Kanda, M., Polanski, K., Heinig, M., Lee, M., et al. (2020). Cells of the adult human heart. Nature *588*, 466–472.
55. Lindsey, M.L., Bolli, R., Canty, J.M., Du, X.-J., Frangogiannis, N.G., Frantz, S., Gourdie, R.G., Holmes, J.W., Jones, S.P., Kloner, R.A., et al. (2018). Guidelines for experimental models of myocardial ischemia and infarction. Am. J. Physiol. Heart Circ. Physiol. *314*, H812–H838.
56. Dong, Y., Zhuang, X.-X., Wang, Y.-T., Tan, J., Feng, D., Li, M., Zhong, Q., Song, Z., Shen, H.-M., Fang, E.F., and Lu, J.-H. (2023). Chemical mitophagy modulators: Drug development strategies and novel regulatory mechanisms. Pharmacol. Res. *194*, 106835.
57. Raza, S., Jokl, E., Pritchett, J., Martin, K., Su, K., Simpson, K., Birchall, L., Mullan, A.F., Athwal, V.S., Doherty, D.T., et al. (2021). SOX9 is required for kidney fibrosis and activates NAV3 to drive renal myofibroblast function. Sci. Signal. *14*, eabb4282.
58. Bi, W., Jia, J., Pang, R., Nie, C., Han, J., Ding, Z., Liu, B., Sheng, R., Xu, J., and Zhang, J. (2019). Thyroid hormone postconditioning protects hearts from ischemia/reperfusion through reinforcing mitophagy. Biomed. Pharmacother. *118*, 109220.
59. Vives-Bauza, C., Zhou, C., Huang, Y., Cui, M., de Vries, R.L.A., Kim, J., May, J., Tocilescu, M.A., Liu, W., Ko, H.S., et al. (2010). PINK1-dependent recruitment of Parkin to mitochondria in mitophagy. Proc. Natl. Acad. Sci. USA *107*, 378–383.
60. Yamano, K., Kikuchi, R., Kojima, W., Hayashida, R., Koyano, F., Kawawaki, J., Shoda, T., Demizu, Y., Naito, M., Tanaka, K., and Matsuda, N. (2020). Critical role of mitochondrial ubiquitination and the OPTN-ATG9A axis in mitophagy. J. Cell Biol. *219*, e201912144.
61. Bøtker, H.E., Hausenloy, D., Andreadou, I., Antonucci, S., Boengler, K., Davidson, S.M., Deshwal, S., Devaux, Y., Di Lisa, F., Di Sante, M., et al. (2018). Practical guidelines for rigor and reproducibility in preclinical and clinical studies on cardioprotection. Basic Res. Cardiol. *113*, 39.
62. Zhou, H., Zhang, Y., Hu, S., Shi, C., Zhu, P., Ma, Q., Jin, Q., Cao, F., Tian, F., and Chen, Y. (2017). Melatonin protects cardiac microvasculature against ischemia/reperfusion injury via suppression of mitochondrial fission-VDAC1-HK2-mPTP-mitophagy axis. J. Pineal Res. *63*, e12413.
63. Huang, S., Li, Z., Wu, Z., Liu, C., Yu, M., Wen, M., Zhang, L., and Wang, X. (2021). DDAH2 suppresses RLR-MAVS-mediated innate antiviral immunity by stimulating nitric oxide-activated, Drp1-induced mitochondrial fission. Sci. Signal. *14*, eabc7931.
64. Zhou, H., Wang, J., Hu, S., Zhu, H., Toanc, S., and Ren, J. (2019). BI1 alleviates cardiac microvascular ischemia-reperfusion injury via modifying mitochondrial fission and inhibiting XO/ROS/F-actin pathways. J. Cell. Physiol. *234*, 5056–5069.
65. Luo, C., Zhang, Y., Guo, H., Han, X., Ren, J., and Liu, J. (2020). Ferulic Acid Attenuates Hypoxia/Reoxygenation Injury by Suppressing Mitophagy Through the PINK1/Parkin Signaling Pathway in H9c2 Cells. Front. Pharmacol. *11*, 103.
66. Roshanzadeh, A., Oyunbaatar, N.-E., Ganjbakhsh, S.E., Park, S., Kim, D.-S., Kanade, P.P., Lee, S., Lee, D.-W., and Kim, E.-S. (2021). Exposure to nanoplastics impairs collective contractility of neonatal cardiomyocytes under electrical synchronization. Biomaterials *278*, 121175.
67. Alghanem, A.F., Wilkinson, E.L., Emmett, M.S., Aljasir, M.A., Holmes, K., Rothermel, B.A., Simms, V.A., Heath, V.L., and Cross, M.J. (2017). RCAN1.4 regulates VEGFR-2 internalisation, cell polarity and migration in human microvascular endothelial cells. Angiogenesis *20*, 341–358.
68. Liu, Z., Gan, L., Xu, Y., Luo, D., Ren, Q., Wu, S., and Sun, C. (2017). Melatonin alleviates inflammasome-induced pyroptosis through inhibiting NF-κB/GSDMD signal in mice adipose tissue. J. Pineal Res. *63*, e12414.

STAR★METHODS

KEY RESOURCES TABLE

REAGENT or RESOURCE	SOURCE	IDENTIFIER
Antibodies		
LC3B	Abcam	Cat#ab192890; RRID: AB_2827794
TOMM20	Abcam	Cat#ab186735; RRID: AB_2889972
Parkin	Abcam	Cat#ab77924; RRID: AB_1566559
VDAC1	Abclonal	Cat#A19707; RRID: AB_2862746
PINK1	Abclonal	Cat#A11435; RRID: AB_2758558
PHB2	Abclonal	Cat#A4504; RRID: AB_2765720
β-Actin	Abclonal	Cat#AC026; RRID: AB_2768234
Chemicals, peptides, and recombinant proteins		
Corosolic acid	MedChemExpress	Cat#HY-N0280
Triphenyltetrazolium chloride	solarbio	Cat#G3005
Evans blue	Shyuanye	Cat#R20616
DAPI solution	Beyotime	Cat#C1002
GP-transfect-Mate	Gene-Pharma	Cat#G04008
Other		
H&E Staining kit	Beyotime	Cat#C0105S
CCK-8	Dojindo	Cat#CK04
LDH kit	Beyotime	Cat#C0016
Enhanced ATP Assay Kit	Beyotime	Cat#S0027
MDA Kit	Beyotime	Cat#S0131S
TUNEL apoptosis assay kit	Beyotime	Cat#C1088
Mitochondrial isolation reagents	Beyotime	Cat#C3601 and C3606
MitoSOX™ Red	Invitrogen	Cat#M36008
ROS kit	Beyotime	Cat#S00635
JC-1 kit	Beyotime	Cat#C2003
Mito-Tracker Red CMXRos	Beyotime	Cat#C1035
Mito-Tracker Green	Beyotime	Cat#C1048
LysoTracker red	Beyotime	Cat#C1046
Oxygen Consumption Rate Plate Assay Kit	Dojindo	Cat#E297
Wheat germ agglutinin (WGA)	Sigma	Cat#L4895

RESOURCE AVAILABILITY

Lead contact

Further information and requests for resources and reagents should be directed to and will be fulfilled or facilitated by the lead contact Hongxia Li (shrimp@suda.edu.cn).

Materials availability

This study did not generate new unique reagents.

Data and code availability

- Data: The data sources of this study are presented in the ''STAR methods'' sections.
- Code: This paper does not report the original code.

- All data related to our conclusions in current study are presented in the main text and/or supplemental information. Additional data related to this article is available from the lead contact upon request.

EXPERIMENTAL MODEL AND STUDY PARTICIPANT DETAILS

Animals

Male Sprague-Dawley rats, weighing between 250 and 300 g, about 8 weeks old, were purchased from Shanghai Slaughter Laboratory Animals Co. The rats were housed at room temperature of 22°C–24°C and relative humidity of about 50%, 4 rats per cage, fed with sterile water and standard chow, in accordance with the Principles of Laboratory Animal Ethics and Care and Use of Laboratory Animals of Soochow University.

METHOD DETAILS

Rat model of myocardial I/R injury

All experiments were carried out in accordance with the Soochow University's ethical committee's standards for using animals in research. Four groups of adult male Sprague-Dawley (SD) rats (aged 8–12 weeks and weighing 270 ± 20 g) were created at random: Sham+DMSO group, Sham+CA group, I/R + DMSO group, and I/R + CA group. In agreement with prior work, rats were administered corosolic acid (10 mg/kg/d) or DMSO 14 days prior to myocardial I/R damage. Corosolic acid (MedChemExpress, HY-N0280) was administered via intraperitoneal injection with DMSO as the vehicle. After 14 days, the rats were subjected to myocardial ischemia for 45 min and then reperfusion for 120 min. Specifically, we used a standard limb II lead electrocardiogram for continuous monitoring of the rats throughout the experiment. The tracheal incision and intubation were performed, then connected to a mechanical ventilator for ventilation support. Subsequently, a left thoracic incision was made, and a 6-0 silk thread was carefully ligatured the root of the anterior descending branch of the left coronary artery (LAD), precisely positioned 2 mm below the intersection of the left atrial appendage and arterial conus. Following a period of 45 min of induced ischemia, the slip-knot was untied, initiating a 120 min reperfusion phase.[55,61] The same thoracotomy technique was carried out in the sham group, but the coronary arteries were not strangulated.

TTC and Evans blue staining

At the end of the perfusion of the rat heart, the coronary artery was ligated at the original ligation site, and the heart was clipped at the root of the aorta and rinsed clean with PBS. Next, 2 mL of 1% Evans Blue solution was drawn up with a syringe and slowly injected into the aortic root, and the heart was observed to turn blue, repeated 3–4 times to ensure adequate staining. Subsequently, the hearts were rinsed twice with PBS, and the stained hearts were placed in a refrigerator at −20°C for 30 min. The frozen hearts were removed, and five slices of approximately 2 mm thickness were cut along the long axis of the left ventricle from the apex to the base of the heart, and the slices were placed at room temperature to rewarm. After the slices were returned to room temperature, they were carefully placed in 1% TTC solution, allowing the solution to fully cover the slices, and placed in a 37°C thermostat for 15 min. At the end of staining the sections were washed with PBS and then fixed in 4% paraformaldehyde solution overnight. The next day pictures were taken with a camera for subsequent analysis.

Transthoracic echocardiography

Two-dimensional echocardiography was performed in rats utilizing a Vivid 7 Dimension (GE Medical system). An independent observer who was not aware of the treatment groups captured and later examined the parasternal short-axis echocardiographic pictures. Left ventricular ejection fraction (LVEF) and left ventricular fractional shortening (LVFS) were measured.

Transmission electron microscopy

Cardiac tissues were fixed with 2.5% glutaraldehyde for 2–3 h at room temperature and then placed at 4°C. 0.1M phosphate buffer PB (PH7.4) formulated with 1% OsO4 acid was fixed for 2 h at room temperature away from light. Tissues were fixed in 1% OsO4 in 0.1M phosphate buffer PB (PH7.4) for 2 h at room temperature away from light. After the tissue had undergone gradient dehydration, acetone and EMBed 812 were applied for penetration for 4, 16, and 6 h at a ratio of 1:1, 1:2, and 0:1, respectively. The samples were placed in EMBed 812 overnight at 37°C and then placed in a 60°C oven for 48 h. An ultrathin slicer (Leica UC7) was used to slice the resin blocks into sections that were between 60 and 80 nm thick. Stained with 2% uranium acetate saturated alcohol solution and 2.6% Lead citrate staining in turn.[62–64] After being dried by the filer paper, sections dried overnight at room temperature. Observed under an HT-7800 transmission electron microscope (HITACHI).

Hematoxylin and Eosin (H&E) staining

Taken advantage of standard methods to fix the heart tissues in 4% paraformaldehyde and embed them in paraffin. The tissue sections were deparaffinized, then rehydrated, and H&E staining was done. A light microscope (NIKON ECLIPSE E100) was used to capture the images.

Immunofluorescence and immunohistochemistry

Myocardial tissues were fixed with 4% paraformaldehyde for 24 h and embedded in paraffin. The tissue blocks were cut into 4-μm-thick sections. Then, the sections were dewaxed and rehydrated for immunofluorescence and immunohistological staining. Cells were fixed with 4%

paraformaldehyde for 15 min, followed by permeabilization with 0.5% Triton X-100 for 10 min. It was then blocked with 3% BSA for 1 h at room temperature. After removing the sealing solution, the sections were covered with a drop of primary antibody and stored at 4°C overnight. After three washes with phosphate-buffered saline (PBS), the cells were incubated with secondary antibodies for 1 h in the dark. Images are captured under a microscope (NIKON ECLIPSE E100). The primary antibodies utilized in the present experiment were as follows: LC3B (1:150, Abcam, #ab192890), PINK1 (1:100, Abclonal, #A11435), Parkin (1:300, Servicebio, #GB114834).

CCK-8 and LDH

Cytotoxicity was assessed using Cell Counting Kit-8 (CCK-8) (CK04, Dojindo, Japan). 10 μL of CCK-8 solution was added to 100 μL of culture medium for dilution. After continued incubation for 1 h in the cell incubator, the optical density was measured at 450 nm using a microplate reader (Thermo Fisher Scientific). Moreover, cytotoxicity was evaluated by the Lactate dehydrogenase (LDH) Cytotoxicity Assay Kit (C0016, Beyotime, China). The absorbance of each well was measured at 490 nm and 600 nm in accordance with the manufacturer's instructions.

Quantification of ATP and MDA

ATP levels were measured utilizing the Enforced ATP Assay Kit (S0027, Beyotime, China). Sample extracts and standards were applied to a 96-well fluorescence detection plate referring to the directions, followed by the addition of reaction buffer. The absorbance of each well at 562 nm was obtained via a microplate reader (Thermo Fisher Scientific). Calculate the ATP content in the samples according to the standard curve. Malondialdehyde (MDA) levels were detected using a lipid oxidation detection kit (S0131S, Beyotime, China), as evidenced by absorbance at 532 nm.

Serum levels of BNP and cTnT

After I/R, blood samples were taken, and serum was extracted by centrifuging at 2000×g for 20 min. The ELISA kit (LunChangshuo Biotech, China) was used to determine the level of cardiac troponin T (cTnT) and brain natriuretic peptide (BNP) in accordance with the manufacturer's instructions.

TUNEL staining

The rate of apoptosis was identified utilizing the TUNEL Apoptosis Assay Kit (C1088, Beyotime, China). Specifically, the tissues from reperfused myocardium were gathered and preserved right away with 3.7% paraformaldehyde. Stain the sections according to the instructions. Observe under a fluorescent microscope (NIKON ECLIPSE C1).

Cell culture and treatment

H9C2 cells: Rat heart-derived H9C2 cells (Shanghai Institute of Cell Biology, Chinese Academy of Science) were cultured with Dulbecco's modified Eagle's medium (DMEM) containing 10% fetal bovine serum (FBS; 10099141C, Gibco, America), 100 U/mL penicillin, and 100 mg/mL streptomycin (C0222, Beyotime, China) at 37°C with 5% CO_2. The H9C2 cells were treated with a previous method to mimic Hypoxia reoxygenation (H/R) injury.[65] The cell culture medium was altered to a sugar-free medium without FBS and incubated in a pre-mixed gas (94% N_2, 5% CO_2, 1% O_2) incubator for 2 h. After 2 h, the cell culture medium was shifted to a complete medium (10% FBS) and incubated in an atmospheric incubator for 4 h. The control cells were incubated with a complete medium of 10% FBS in an atmospheric incubator for 6 h. Two concentrations of CA (10 or 15 μM, MedChemExpress, HY-N0280) were preadministered for 24 h.

Neonatal rat ventricular myocytes (NRVMs): The left ventricle of 1-2-day-old Sprague-Daley rats (Animal Experiment Center of Soochow University, Suzhou, China) was collected. Myocardium was washed three times with D-Hanks solution. D-Hanks solution was poured off, and the myocardium was clipped into small particles, added 0.025% trypsin and placed at 4°C overnight. At room temperature, the tissue was gently blown using a 25 mL wide-mouth pipette. The same volume of Hanks solution (containing calcium and magnesium) as the trypsin was added to the centrifuge tube. Next, collagenase was added to the solution. The solution was shaken in a water bath at 37°C for 50 min. The solution was then centrifuged at 1000 rpm for 5 min to remove the supernatant. The appeal procedure was repeated after 20 mL D-Hanks solution was added to the precipitate. Precipitated cells were resuspended in a medium with 10% FBS and bromodeoxyuridine (BrdU, 0.1 mM). The dishes were incubated in a 37°C incubator for 1.5 h to remove fibroblasts. The supernatant was transferred to a new culture dish. And after 24 h, the NRVMs were used for subsequent experiment.[66] Similarly, NRVMs are also used to build the H/R injury model.

Small interfering RNA (siRNA) transfection

Shanghai Gene-Pharma Co. created and offered the siRNA against PHB2. The RNAi sequences were as follows: siRNA-PHB2: 5′-CCGUGAGUCCGUAUUCACUTT-3′; anti-sense: 5′-AGUGAAUACGGACUCACGGTT-3′, siRNA-Ctrl: 5′-UUCUCCGAACGUGUCACGUTT-3′; anti-sense: 5′-ACGUGACACGUUCGGAGAATT-3′. The siRNA was transfected into cardiomyocytes using GP-transfect-Mate (Gene-Pharma, Inc., Shanghai, China).[67] The cardiomyocytes were collected after 48–72 h, and western blotting and qPCR were utilized to confirm the knockdown effectiveness.[68]

Mitochondrial isolation

Tissue and cell samples were homogenized by a homogenizer after addition of mitochondrial isolation reagents (C3601 and C3606, Beyotime, China) according to the product manual. Afterward, the homogenate was centrifuged at 600 × g, at 4°C for 10 min. The supernatant is then centrifuged at 11000 × g for 10 min at 4°C.

Western blotting

The lysates were collected and centrifuged at 12,000 × g for 15 min at 4°C. After adding the loading buffer to the supernatant, boil it at 95°C for 15 min. Using a 10–15% SDS-PAGE, 20 μg of proteins were separated, and then they were transferred to PVDF membranes. Then, the PVDF membrane was blocked with 5% BSA for 1 h at room temperature. The membrane was immersed in diluted primary antibody solution and incubated overnight at 4°C. The secondary antibody was added after four washes using a TBST shaker and incubated for 2 h at room temperature. Four washes were followed by imaging using a gel imager (Bio-Rad, CA). Quantification of each protein band was performed using the ImageJ analysis program version 1.8.0. Next, the ratio of the peak area of the target protein to the peak area of the corresponding internal reference was calculated to produce a set of data. The average of the three experiments for the control group was calculated and normalised by dividing all the data from the previous step by this average to obtain the final results of the Western blots. The following were the primary antibodies used for immunoblotting: LC3B (1:2000, abcam, #ab192890), TOMM20 (1:2000, abcam, #ab186735), VDAC1 (1:1000, Abclonal, #A19707), PINK1 (1:1000, Abclonal, #A11435), Parkin (1:2000, abcam, #ab77924), PHB2 (1:1000, Abclonal, #A4504).

ROS staining and mitochondrial membrane potential measurement

Oxidative stress accumulation in cells was detected using the cytoplasmic ROS probe fluorescence 2′,7′-dichlorofluorescein diacetate (DCFH-DA) (10 μmol/L, S0033M, Beyotime, China) and Dihydroethidium (DHE) (5 μmol/L, S0063, Beyotime, China). H9C2 cells were cultured at the same density in six-well plates, and after two washes with PBS, they were incubated with DCFH-DA probe or Dihydroethidium probe for 30 min at 37°C protected from light. Fluorescence images were then recorded using a fluorescence microscope after the cells were washed twice with PBS. Mitochondrial ROS levels and mitochondrial membrane potential measurements were achieved by staining NRVMs cultured at the same density on 24-well crawls. Cells were washed using PBS and then stained with the mitochondrial ROS indicator MitoSOX Red (2 μmol/L, M36008, Invitrogen, America) and the mitochondrial membrane potential probe JC-1 (C2003, Beyotime, China), respectively, for 20 min at 37°C. Next, recordings were made by fluorescence microscopy after two washes using PBS.

Measurement of oxygen consumption rate (OCR)

H9C2 cells were plated into each well of a 96-well plate and cultured for 24 h. OCR was measured according to the instruction manual of the Extracellular OCR Plate Assay Kit (E297, Dojindo, Japan). The cells were treated with either control DMEM or working solution for 30 min, and the fluorescent signals were measured at 10 min intervals. The calculation of OCR was derived from an analysis of the kinetic profiles obtained from measurements.

Molecular docking

The 3D structure of CA was downloaded from PubChem data, and then uploaded it into ChemBio3D Ultra 14.0 for energy minimization. The Minimum RMS Gradient was installed to 0.001. Next, the protein structure of PHB2 was downloaded from the UNIPROT database, and protein crystal water and original ligands were eliminated by PyMOL2.3.0. The protein structure was input into AutoDocktools (v1.5.6) for hydrogenation, charge calculation, charge assignment, and atom type assignment. Protein binding sites were predicted by POCASA 1.1, the docking was implemented through AutoDock Vina1.1.2. In the course of the above, PHB2 related parameters were set as: center_x = −14.5, center_y = −14.0, center_z = 9.6; search space: size_x:60, size_y: 60, size_z:60 (the distance between each grid point is 0.375 Å), exhaustiveness:10, the rest parameters are set by default. PyMOL2.3.0 and Discovery Studio 2019 were employed for evaluating the interaction mode of the docking data.

Statistical analysis

Data from at least three different experiments were expressed as the mean ± standard deviation. Statistical analysis (GraphPad Prism 9.0 software) evaluated the differences between groups by one-way ANOVA or two-way ANOVA. The signs of statistical significance are $*p < 0.05$, $**p < 0.01$, $***p < 0.001$, $****p < 0.0001$, ns represent not significant.